

TU-604  
 DPNU-00-34  
 hep-ph/0010260  
 October, 2000

# Top Mode Standard Model with Extra Dimensions

Michio HASHIMOTO\*, Masaharu TANABASHI†

*Department of Physics, Tohoku University  
 Sendai 980-8578, Japan*

Koichi YAMAWAKI‡

*Department of Physics, Nagoya University  
 Nagoya 464-8602, Japan*

## Abstract

We critically examined a version of the top mode standard model recently cast in the extra dimensions by Arkani-Hamed et al., based on the (improved) ladder Schwinger-Dyson (SD) equation for the  $D (= 6, 8)$ -dimensional gauge theories. We found that the bulk QCD cannot have larger coupling beyond the *non-trivial ultraviolet (UV) fixed point*, the existence of which is supported by a recent lattice analysis. The coupling strength at the fixed point is evaluated by using the one-loop renormalization group equation. It is then found that, in a version with only the third family (as well as the gauge bosons) living in the  $D$ -dimensional bulk, the critical (dimensionless) coupling for the dynamical chiral symmetry breaking to occur is larger than the UV fixed point of the bulk QCD coupling for  $D = 6$ , while smaller for  $D = 8$ . We further found that the *improved* ladder SD equation in  $D$  dimensions has an *approximate scale-invariance* due to *running* of the coupling and hence has an *essential-singularity scaling* of the “conformal

---

\*michioh@tuhep.phys.tohoku.ac.jp

†tanabash@tuhep.phys.tohoku.ac.jp

‡yamawaki@eken.phys.nagoya-u.ac.jp

phase transition”, similarly to the Miransky scaling in the four-dimensional *ladder* SD equation with *non-running* coupling. This essential-singularity scaling can resolve the fine-tuning even when the cutoff (“string scale”) is large. Such a theory has a *large anomalous dimension*  $\gamma_m = D/2 - 1$  and is expected to be free from the flavor-changing-neutral-currents problem as in the walking technicolor for  $D = 4$ . Furthermore the induced bulk Yukawa coupling becomes finite even at infinite cutoff limit (in the formal sense), similarly to the renormalizability of the gauged Nambu-Jona-Lasinio model. Comments are made on use of the “effective” coupling, which includes finite renormalization effects, instead of the  $\overline{MS}$  running coupling in the improved ladder SD equation.

# 1 Introduction

The top quark condensate proposed by Miransky, Tanabashi and Yamawaki (MTY) [1, 2] and by Nambu [3] independently is a natural idea to account for the large mass of the top quark ( $t$ ) on the weak-scale order in contrast to other quarks and leptons. The Higgs boson in the standard model (SM) emerges as a  $\bar{t}t$  bound state and hence is deeply connected with the top quark itself. Thus the model may be called “top mode standard model (TMSM)” [2].

Actually, MTY introduced explicit four-fermion interactions [1, 2]

$$\mathcal{L}_{4f} = \frac{4\pi^2}{N_c \Lambda^2} \left[ g_t (\bar{\psi}_L t_R)^2 + g_b (\bar{\psi}_L b_R)^2 + g^{(2)} \epsilon^{i,k} \epsilon^{j,l} (\bar{\psi}_L^i \psi_R^j) (\bar{\psi}_L^k \psi_R^l) + \text{h.c.} \right], \quad (1.1)$$

with  $i(j, k, l) = t, b$  for top and bottom quarks, where  $g_t, g_b, g^{(2)}$  are dimensionless four-fermion couplings,  $\Lambda$  is the cutoff and  $N_c$  the number of colors, and similarly for leptons as well as the first and second generations of quarks and leptons. While  $g_t$  is responsible for the top mass, the  $g^{(2)}$  coupling is vital to the generation of the bottom mass without problem of the axion. MTY further gave a concrete formulation based on the (improved) ladder Schwinger-Dyson (SD) equation for the QCD plus the four-fermion interaction (1.1), the gauged Nambu-Jona-Lasinio (NJL) model, and found that when

$$g_t > g_{crit} > g_b, \quad (1.2)$$

only the top quark can condense giving rise to the large top mass while the bottom quark is kept massless, where  $g_{crit}$  is the critical coupling of the SD equation. As to the value of the top mass, MTY plugged the solution of the (improved) ladder SD equation into the Pagels-Stokar (PS) formula [4] for  $F_\pi = 250\text{GeV}$  and predicted  $m_t \simeq 250\text{GeV}$  for the cutoff near the Planck scale [1, 2].

The model was further formulated in an elegant fashion by Bardeen, Hill and Lindner (BHL) [5] in the SM language, based on the renormalization-group equation (RGE) and the compositeness condition. It essentially incorporates  $1/N_c$  sub-leading effects disregarded by the MTY paper. BHL is in fact equivalent to MTY at  $1/N_c$ -leading order [6]. Such  $1/N_c$ -subleading effects reduced the above MTY value 250 GeV down to 220 GeV, a somewhat smaller value but still on the order of the weak scale. Even this value, however, turned out to be a bit larger than the mass of the later observed top quark.

Quite recently, Arkani-Hamed, Cheng, Dobrescu and Hall (ACDH) [7] proposed a very interesting version of the TMSM in six and eight dimensions, in which the third family fermion and the gauge bosons are put in the  $D (= 6, 8)$ -dimensional bulk, while first and second families are in the four-dimensional brane (3-brane). Then they argued that the  $D$ -dimensional SM gauge couplings become strong due to Kaluza-Klein (KK) modes of the standard model gauge bosons and hence may naturally give rise to the effective four-fermion interactions *in D-dimensional bulk* which have the same structure as Eq.(1.1), with  $g_t > g_{crit} > g_b$ , the situation similar to the original TMSM,

Eq.(1.2). Moreover they argued that the top mass can be arranged to be a realistic value due to the effects of many KK modes of top quark even for the TeV scale cutoff, thus the model may be free from serious fine tuning as compared with the original TMSM having the cutoff near the Planck scale. The model is largely based on the earlier papers [8, 9] on the proposal of formulating the top quark condensate in the extra dimensions in the spirit of large scale compactification scenarios [10, 11]<sup>1</sup>.

However, ACDH gave no dynamical arguments on whether the dynamical symmetry breaking really takes place or not in their model. Actually, they made an ansatz that bulk strong gauge dynamics in the ultraviolet region near the cutoff (“string scale”) can well be simulated by the  $D$ -dimensional *bulk four-fermion couplings* characterized by the cutoff scale. They then calculated *relative strength* of the bulk attractive forces among various channels based on the Most Attractive Channel (MAC) hypothesis [14] and argued that only the top coupling can be arranged to be above the critical coupling as Eq.(1.2) in the original mechanism of MTY. However, it would make sense only when these four-fermion couplings are near the critical coupling, the situation being what they simply assumed. Actually, there is no information on the strength of the bulk effective four-fermion couplings which cannot be related in any definite manner to the bulk gauge coupling, while the latter is calculable through matching with the low-energy SM coupling in four dimensions (3-brane) at the compactification scale [15].

In this paper, we shall study the dynamical issues of the ACDH version of the TMSM, based on the (improved) ladder SD equation for the gauge theories in the bulk  $D (= 6, 8)$  dimensions. As in ACDH [7] we here assume that the bulk anomaly may be cancelled by some stringy arguments like the Green-Schwarz mechanism. Then we present explicit solutions for the dynamical chiral symmetry breaking ( $D\chi$ SB) for  $D$  dimensions with their implications on the ACDH scenario and reveal some salient features of this dynamics for  $D$  dimensions.

We first discuss a *non-trivial ultraviolet (UV) fixed point* in the one-loop renormalization group equation of the “truncated KK” effective theory [15] of the  $D$ -dimensional non-Abelian gauge theories with the compactified extra dimensions, in a manner similar to the analysis of  $D = 4 + \epsilon$  ( $0 < \epsilon \ll 1$ ) gauge theories. Although such a fixed point cannot be justified for  $\epsilon \sim \mathcal{O}(1)$  within the perturbative analysis, its existence is supported by a recent lattice calculation[26]. Assuming the non-perturbative existence of such a fixed point, we then evaluate the gauge coupling strength at the fixed point by using one-loop RGE which was actually adopted by ACDH for their prediction of the top quark mass. In the bulk SM, QCD is the only non-Abelian gauge theory relevant to the  $D\chi$ SB. We then observe that the  *$D$ -dimensional bulk QCD coupling cannot grow over the fixed point value*, since at a certain compactification scale we match the bulk QCD coupling with the 3-brane QCD coupling which is obviously small, and hence the phase must be in the weak coupling regime below the fixed point. The QCD coupling for the ACDH version of the TMSM for  $D = 6, 8$  is actually evaluated by the truncated

---

<sup>1</sup> The previous studies in the extra dimensions[8, 9, 12] were focused on the four-fermion interactions in the 3-brane in contrast to those in the ACDH which are *in the  $D$ -dimensional bulk* [7, 13].

KK effective theory.

We next study the dynamical symmetry breaking in  $D$ -dimensional gauge theories, based on the improved ladder SD equation [16], with the  $D$ -dimensional bulk gauge coupling in the ladder SD equation being simply replaced by the  $(\overline{MS})$  one-loop running coupling. Actually, in  $D$ -dimensional gauge theories for both the fermion and the gauge bosons living in the  $D$ -dimensional bulk, with the extra dimensions being compactified, *the dynamical symmetry breaking can be triggered only by the dynamics in the ultraviolet region* where the gauge coupling becomes strong, and hence can be well described by the  $D$ -dimensional improved ladder SD equation, with *massless gauge bosons in  $D$ -dimensional bulk, irrespectively of details of the infrared dynamics of the compactification scale*.

It is then found that, for the simplest version of the ACDH scenario with only the third family (as well as the gauge bosons) living in the bulk, the UV fixed point of the bulk QCD coupling is smaller than the critical coupling for the dynamical chiral symmetry breaking to occur for  $D = 6$ , while it is opposite for  $D = 8$ . Namely, *the dynamical symmetry breaking due to the bulk QCD dynamics cannot take place in 6 dimensions and can in 8 dimensions for the simplest ACDH version of the TMSM*.

Remarkably enough, the improved ladder SD equation with *running* coupling has approximately *scale-invariant form* in  $D$  dimensions and thus *the scaling law is the essential-singularity type of “conformal phase transition”* [17] similar to the Miransky scaling in the four-dimensional ladder SD equation with the *non-running* coupling [18].

Moreover, it has a *large anomalous dimension*  $\gamma_m = D/2 - 1$  near the fixed point and hence has a chance to solve the flavor-changing-neutral current (FCNC) problem like in the walking technicolor for  $D = 4$  [19].

This corresponds to the slowly damping mass function which still yields finiteness of the bulk decay constant  $F_\pi^{(D)}$  and hence of the induced bulk Yukawa coupling even in the limit of infinite cutoff (in the formal sense). Such a situation is similar to the renormalizability of the gauged NJL model in four dimensions [20].

We also comment on that, instead of the  $\overline{MS}$  running coupling in the improved ladder SD equation, we may use the “effective” coupling including finite renormalization effects. Unlike the  $\overline{MS}$  coupling, the “effective” gauge coupling includes the effects of KK modes heavier than the renormalization scale. It is shown that the decoupling theorem is violated in the “effective” gauge coupling due to the summation of the large number of KK modes. Nevertheless we find an *upper bound* on the effective gauge coupling strength, which is roughly proportional to the UV fixed point in the  $\overline{MS}$  scheme. We also show that the upper bound of the “effective” gauge coupling can be regarded as a UV fixed point of “bare gauge coupling”. Our results are therefore unchanged qualitatively even if we adopt the “effective” coupling instead of  $\overline{MS}$ .

It should be emphasized, however, that the finite renormalization can affect our quantitative results, such as the value of the critical coupling. Actually the effective coupling tends to be stronger than the  $\overline{MS}$  coupling and hence there appears a possibility that the bulk SM couplings could lead to the top quark condensate in the manner

of Eq.(1.2) under certain conditions even for  $D = 6$  in the simplest ACDH version of the TMSM.

The paper is organized as follows: In Section 2 we discuss existence of the non-trivial UV fixed point in  $D(= 4 + \epsilon)$ -dimensional non-Abelian gauge theories in the  $\epsilon$  expansion. Then we show the non-trivial UV fixed point in the  $D(= 4 + \delta)$ -dimensional non-Abelian gauge theories with the extra  $\delta(= 2, 4)$  dimensions compactified. The value of the UV fixed point for the ACDH version of the TMSM is evaluated for  $D = 6, 8$  based on the truncated KK effective theory. We then give a rough argument why the “strong” bulk QCD coupling may not necessarily give rise to the condensate, based on the naive dimensional analysis (NDA) [21, 22]. In Section 3 we derive the  $D$ -dimensional ladder SD equation, and also the improved ladder SD equation. In Section 4 we find numerically the critical values of the  $D\chi$ SB to occur for  $D = 6, 8$ , which are compared with those of the ACDH couplings estimated in Section 2. Also the analytical solution is obtained in further approximation, which shows essential-singular-type scaling. In Section 5 we analyze the Operator Product Expansion (OPE) for the fermion propagator and identify the anomalous dimension which is then calculated to be  $\gamma_m = D/2 - 1$ . In Section 6 the chiral fermion through the orbifold projection into the 3-brane is studied in some details. In Section 7 we discuss use of the effective coupling instead of the  $\overline{MS}$  running coupling in the improved ladder SD equation. Section 8 is devoted to the summary and discussions. Appendix A contains formulas for the angular integration of the ladder SD equation, which is the generalization of the previous result [23] to the arbitrary (non-integer)  $D$  dimensions. Appendix B shows a gap equation of the NJL-type four-fermion model in  $D(> 4)$  dimensions, in which the scaling law is  $1/g_{crit} - 1/g \sim (m/\Lambda)^2$ , essentially the same (up to logarithm) as the NJL model for  $D = 4$ , in sharp contrast to the case of  $D < 4$  where the scaling law is given by  $1/g_{crit} - 1/g \sim (m/\Lambda)^{D-2}$  [24]. Appendix C is for the approximation to the effective coupling discussed in Section 7.

## 2 Existence of ultraviolet fixed point

In order to illustrate existence of the non-trivial ultraviolet fixed point of the gauge theory in more than four dimensions, we start with a brief review of the gauge dynamics in  $D(= 4 + \epsilon, 0 < \epsilon \ll 1)$  dimensions [25] ( $\epsilon$  expansion).

The one-loop renormalization group equation (RGE) of the gauge coupling is given by

$$\mu \frac{d}{d\mu} \hat{g} = \frac{\epsilon}{2} \hat{g} + \frac{b_{(1)}}{(4\pi)^2} \hat{g}^3, \quad (2.1)$$

where  $\hat{g}$  is the dimensionless gauge coupling scaled by a renormalization scale  $\mu$ :

$$g_D \equiv \frac{\hat{g}}{\mu^{\epsilon/2}}, \quad (2.2)$$

with  $g_D$  being the gauge coupling in  $D (= 4 + \epsilon)$  dimensions and of mass dimension  $-\epsilon/2$ . Hereafter we assume that the renormalization-group coefficient  $b_{(1)}$  is negative,  $b_{(1)} < 0$ . From Eq.(2.1), the renormalization-group flow of the dimensionless coupling  $\hat{g}$  is given by

$$\hat{g}^2(\mu) = \frac{1}{\left(\frac{\mu'}{\mu}\right)^\epsilon \frac{1}{\hat{g}^2(\mu')} - \frac{2}{\epsilon} \frac{b_{(1)}}{(4\pi)^2} \left[1 - \left(\frac{\mu'}{\mu}\right)^\epsilon\right]}. \quad (2.3)$$

We then find an ultraviolet ( $\mu \rightarrow \infty$ ) fixed point

$$g_*^2 = \lim_{\mu \rightarrow \infty} \hat{g}^2(\mu) = \frac{\epsilon (4\pi)^2}{2 - b_{(1)}}. \quad (2.4)$$

It should be emphasized that  $\epsilon$  is considered to be small here and therefore the fixed point  $g_*^2 \propto \epsilon$  is still in its perturbative regime. It is straightforward to extend the analysis to include higher-loop effects. The UV fixed point in the two-loop RGE

$$\mu \frac{d}{d\mu} \hat{g} = \frac{\epsilon}{2} \hat{g} + \frac{b_{(1)}}{(4\pi)^2} \hat{g}^3 + \frac{b_{(2)}}{(4\pi)^4} \hat{g}^5 \quad (2.5)$$

is given in terms of the  $\epsilon$ -expansion,

$$g_*^2 = \frac{(4\pi)^2 \epsilon}{-b_{(1)} 2} \left(1 + \frac{b_{(2)}}{b_{(1)}^2} \frac{\epsilon}{2}\right) + \mathcal{O}(\epsilon^3). \quad (2.6)$$

The two-loop effect,  $b_{(2)}$  term, affects the coefficient of  $\epsilon^2$ , keeping the coefficient of  $\epsilon^1$  unchanged. Actually the  $n$ -loop effect can be regarded as an  $\mathcal{O}(\epsilon^n)$  effect in the  $\epsilon$  expansion. The perturbative stability of the fixed point  $g_*$  is thus guaranteed in the  $D = 4 + \epsilon$  dimensional gauge theories. We also note that the coefficients  $b_{(1)}$  and  $b_{(2)}$  are both negative in QCD with  $N_f \leq 8$ . The two-loop UV fixed point Eq.(2.6) is thus smaller than the one-loop estimate Eq.(2.4).

Hence we expect that there exist (at least) two phases separated by the fixed point  $g_*$  in this theory: The weakly interacting phase  $\hat{g} < g_*$  can be controlled perturbatively. It is therefore considered to be in the Coulomb phase and the chiral symmetry is not broken in this phase. On the other hand, the theory becomes strongly interacting at the low energy region in the phase  $\hat{g} > g_*$ . It is therefore expected to be in the confinement phase and the chiral symmetry is expected to be broken dynamically.

Although the existence of such a fixed point for larger  $\epsilon \sim \mathcal{O}(1)$  cannot be justified within the perturbative analysis, recent analysis based on the lattice gauge theory [26] suggests that the fixed point structure described above holds even in larger (integer) value of  $\epsilon$ , if the extra dimensions are compactified in a short distance.<sup>2</sup> Actually, as

---

<sup>2</sup> There still exists non-trivial phase structure even in the case of non-compactified extra dimensions. However, the phase transition is shown to be first order [27] and we cannot obtain hierarchy between the cutoff scale and the low energy scales.

we will see in the following, there exists a close correspondence between the RGEs of  $\epsilon \ll 1$  and of the compactified extra dimensions even within the perturbative approach.

Now we evaluate the *non-trivial UV fixed point of the gauge theory in  $D (= 4 + \delta)$  dimensions where the extra  $\delta$  dimensions are compactified*. In this case we would need to deal with infinite number of “Kaluza-Klein” (KK) modes above the compactification scale  $R^{-1}$ . However, the KK-modes heavier than the renormalization scale  $\mu$  are actually decoupled in the RGE. We only need to sum up the loops of KK-modes lighter than  $\mu$ . This approach is called “truncated KK” effective theory [15]. The theory can be fully controlled in this truncated KK effective theory.

The RGE of the gauge coupling ( $g$ ) on the 3-brane is given by

$$(4\pi)^2 \mu \frac{d}{d\mu} g = N_{\text{KK}} b' g^3 \quad (2.7)$$

in the truncated KK effective theory. Here  $N_{\text{KK}}$  stands for the number of KK-modes below the renormalization scale  $\mu$ . The RGE factor  $b'$  is given by

$$b' = -\frac{26 - D}{6} C_G + \frac{\eta}{3} T_R N_f, \quad (2.8)$$

where  $\eta$  represents the dimension of the spinor representation of  $SO(1, D - 1)$ ,

$$\eta \equiv \text{tr}_\Gamma 1 = 2^{D/2} \quad \text{for even } D, \quad (2.9)$$

and  $N_f$  is the number of fermions in the bulk. The group-theoretical factors  $C_G$  and  $T_R$  are given by  $C_G = N$  and  $T_R = 1/2$  for  $SU(N)$  gauge theory.

For sufficiently large  $\mu \gg R^{-1}$ ,  $N_{\text{KK}}$  is estimated as [15]

$$N_{\text{KK}} = \frac{1}{n} \frac{\pi^{\delta/2}}{\Gamma(1 + \delta/2)} (\mu R)^\delta, \quad (2.10)$$

where we have assumed that the extra dimensions are compactified to an orbifold  $T^\delta / Z_n$  with  $Z_n$  being discrete group with order of  $n$ .

The gauge coupling on the 3-brane can be related to the gauge coupling in the  $D$  dimensional bulk  $g_D$  as  $g_D^2 = (2\pi R)^\delta g^2 / n$ . Thus the dimensionless bulk gauge coupling  $\hat{g}$  can be defined à la Eq.(2.2):

$$\hat{g}^2 = \frac{(2\pi R \mu)^\delta}{n} g^2. \quad (2.11)$$

Plugging Eq.(2.11) into Eq.(2.7), we obtain

$$\mu \frac{d}{d\mu} \hat{g} = \frac{\delta}{2} \hat{g} + (1 + \delta/2) \Omega_{\text{NDA}} b' \hat{g}^3, \quad (2.12)$$

with  $\Omega_{\text{NDA}}$  being the loop factor in the NDA [21, 22]:

$$\Omega_{\text{NDA}} \equiv \frac{1}{(4\pi)^{D/2}\Gamma(D/2)}, \quad D = 4 + \delta. \quad (2.13)$$

It is interesting to note a similarity between Eq.(2.1) and Eq.(2.12): The factor  $\epsilon$  in the  $\epsilon$ -expansion corresponds to  $\delta$  in the truncated KK effective theory with a simple replacement of  $b/(4\pi)^2$  by  $(1 + \delta/2)\Omega_{\text{NDA}}b'$ .

The RGE Eq.(2.12) can be easily solved as

$$\hat{g}^2(\mu) = \frac{1}{\left(\frac{\mu'}{\mu}\right)^\delta \frac{1}{\hat{g}^2(\mu')} - \left(\frac{2}{\delta} + 1\right)\Omega_{\text{NDA}}b' \left[1 - \left(\frac{\mu'}{\mu}\right)^\delta\right]}. \quad (2.14)$$

Thus, we find a *non-trivial UV fixed point*

$$g_*^2\Omega_{\text{NDA}} = \frac{1}{-\left(\frac{2}{\delta} + 1\right)b'}. \quad (2.15)$$

It should be noted that the coupling  $\hat{g}^2$  in Eq.(2.14) grows very quickly close to value of the fixed point.

In the ACDH scenario [7] of the TMSM, the top quark interaction responsible for the dynamical electroweak symmetry breaking is assumed to come (mainly) from the bulk QCD interaction. On the other hand, the low energy QCD coupling in the 3-brane is well below its fixed point obviously. ( $\hat{g}^2/g_*^2 \simeq 1.83\alpha/n$  ( $0.72\alpha/n$ ) with  $\alpha \equiv g^2/(4\pi)$  for  $D = 6$  ( $D = 8$ ) at  $\mu = R^{-1}$ .) Thus, Eq.(2.15) can be regarded as *the upper bound of the dimensionless coupling of the bulk QCD*. Actually, in the ACDH scenario for  $D = 6$  the upper bound of the dimensionless QCD coupling is given by

$$C_F\hat{g}^2\Omega_{\text{NDA}} < C_Fg_*^2\Omega_{\text{NDA}} \simeq 0.09, \quad (2.16)$$

where we have used  $\delta = 2$ ,  $\eta = 8$ ,  $C_F = 4/3$ ,  $C_G = 3$  and  $N_f = 2$  in Eqs.(2.8) and (2.15). Even though the value of  $g_*$  can be affected by the higher-loop effects, it is proportional to  $1/(-b')$  for sufficiently large  $-b'$ .<sup>3</sup> Eq.(2.16) implies that although the bulk QCD coupling is generally expected to become “strong” in the region beyond the compactification scale, it is actually *not so strong* as to make the perturbative expansion totally useless. Moreover, an analysis similar to Eq.(2.6) indicates that the value of  $g_*$  of the bulk QCD with  $\delta = 2$  and  $N_f = 2$  tends to be decreased by taking

---

<sup>3</sup> It should be emphasized, however, the higher loop effects cannot be made arbitrarily small even in the large  $-b'(> 0)$  limit. Actually Eq.(2.8) shows that the large  $-b'$  corresponds to large  $C_G$  (and small  $N_f$ ) with  $C_G = N$  for  $SU(N)$  gauge theory. The typical size of  $n$ -loop effect at the fixed point is thus of order  $(Ng_*^2\Omega_{\text{NDA}})^n \sim (N/(-b'))^n \simeq (6/(26 - D))^n$  even in the large  $N$  limit.



Figure 1: Feynman diagram of the SD equation in the ladder approximation. Solid lines with and without a blob represent dressed and bare propagators of fermion ( $S(p)$ ,  $S_0(p)$ ), respectively. The gauge boson propagator ( $D_{MN}$ ) is denoted by a wavy line.

into account the two-loop effects. The estimate Eq.(2.16) can thus be regarded as a conservative one, although we expect sizable higher-loop uncertainty in our estimate.

It is therefore quite *non-trivial whether the bulk QCD can be strong enough to trigger the dynamical electroweak symmetry breaking*. Before starting detailed analysis, it would be helpful to give a simpler discussion from the viewpoint of NDA [21, 22] and MAC [14], which leads to a condition for the dynamical symmetry breaking to take place:

$$C_F \hat{g}^2 \Omega_{\text{NDA}} \gtrsim 1, \quad (2.17)$$

where  $\Omega_{\text{NDA}}$  comes from the loop suppression factor of NDA and  $C_F$  is the quadratic Casimir of the fundamental representation which is from the MAC assumption. Hence Eq.(2.16) suggests that the bulk QCD may not be enough to induce the dynamical electroweak symmetry breaking in the ACDH scenario in six dimensions.

However, the present analysis might be too simple-minded. In the following sections we will investigate this issue using the SD gap equation within the improved ladder approximation.

### 3 Improved ladder Schwinger-Dyson equation

#### 3.1 Ladder SD equation

We next investigate the condition for the chiral symmetry to break dynamically in gauge theories in dimensions  $D > 4$ . The dimensions of the space-time  $D$  need to be even in order that the chiral symmetry is defined in the bulk. Since the electroweak symmetry is a chiral symmetry, the condition studied in this section can be regarded as the condition for the dynamical electroweak symmetry breaking in the bulk.

The bulk dynamical chiral symmetry breaking ( $D\chi\text{SB}$ ) in gauge theories with extra dimensions is considered as nonperturbative effects of the high energy region [7] where the SM gauge couplings in the  $D$ -dimensional bulk become strong. We therefore neglect the infrared dynamics due to the finite size effects of extra dimensions in the following.

The  $D$ -dimensional ladder SD equation for the fermion propagator is given by Fig.1.

It then reads

$$iS^{-1}(p) = iS_0^{-1}(p) + \int \frac{d^D q}{(2\pi)^D i} \left[ -ig_D T^a \Gamma^M \right] S(q) \left[ -ig_D T^a \Gamma^N \right] D_{MN}(p - q), \quad (3.1)$$

where  $S$  and  $S_0$  denote dressed and bare propagators of the fermion, respectively. Within the ladder approximation, the gauge boson propagator  $D_{MN}$  is approximated at the tree-level by the form

$$D_{MN}(p - q) = \frac{-i}{(p - q)^2} \left[ g_{MN} - (1 - \xi) \frac{(p - q)_M (p - q)_N}{(p - q)^2} \right], \quad (3.2)$$

with  $\xi$  being a gauge-fixing parameter. We also indicate the the gamma matrix of  $SO(1, D - 1)$  by  $\Gamma^M$

$$\{\Gamma^M, \Gamma^N\} = 2g^{MN}, \quad M, N = 0, 1, 2, 3, 5, \dots, D. \quad (3.3)$$

Since we are dealing with  $D\chi$ SB in the bulk, we take the bare propagator of fermion in  $D$ -dimension to be massless,  $iS_0^{-1}(p) = \not{p}$ . The dressed propagator  $S$  may be written as

$$iS^{-1}(p) = A(-p^2)\not{p} - B(-p^2). \quad (3.4)$$

Then Eq.(3.1) leads to coupled SD equations after the Wick rotation:

$$\begin{aligned} A(p_E^2) &= 1 + \frac{C_F g_D^2}{p_E^2} \int \frac{d^D q_E}{(2\pi)^D} \frac{A(q_E^2)}{A^2 q_E^2 + B^2} \times \\ &\quad \times \left[ -(3 - D - \xi) \frac{p_E \cdot q_E}{(p_E - q_E)^2} + 2(1 - \xi) \frac{p_E \cdot (p_E - q_E) q_E \cdot (p_E - q_E)}{(p_E - q_E)^4} \right], \end{aligned} \quad (3.5)$$

$$B(p_E^2) = (D - 1 + \xi) C_F g_D^2 \int \frac{d^D q_E}{(2\pi)^D} \frac{B(q_E^2)}{A^2 q_E^2 + B^2} \frac{1}{(p_E - q_E)^2}, \quad (3.6)$$

where  $p_E$  and  $q_E$  denote the Euclidean momenta  $p_E^2 \equiv -p^2$ ,  $q_E^2 \equiv -q^2$ , respectively. Performing the angular integrals in Eq.(3.5) and Eq.(3.6), we find

$$A(x) = 1 + 2 \frac{D - 2}{D} \xi \Omega_{\text{NDA}} \frac{C_F}{x} \int_0^{\Lambda^2} dy y^{D/2-1} \frac{g_D^2 A(y)}{A^2 y + B^2} K_A(x, y), \quad (3.7)$$

$$B(x) = (D - 1 + \xi) \Omega_{\text{NDA}} C_F \int_0^{\Lambda^2} dy y^{D/2-1} \frac{g_D^2 B(y)}{A^2 y + B^2} K_B(x, y), \quad (3.8)$$

with  $x \equiv p_E^2$ ,  $y \equiv q_E^2$ , where we have introduced the ultraviolet cutoff  $\Lambda$ , which is believed to have physical meaning such as the string scale in this class of models with extra dimensions.

The integral kernels  $K_A$  and  $K_B$  are given in Ref. [23] and are explicitly written as

$$K_A(x, y) = \frac{y}{x} \theta(x - y) + (x \leftrightarrow y), \quad (3.9)$$

$$K_B(x, y) = \frac{1}{x} \theta(x - y) + (x \leftrightarrow y), \quad (3.10)$$

for  $D = 4$ , and

$$K_A(x, y) = \frac{y}{x} \left(1 - \frac{y}{2x}\right) \theta(x - y) + (x \leftrightarrow y), \quad (3.11)$$

$$K_B(x, y) = \frac{1}{x} \left(1 - \frac{y}{3x}\right) \theta(x - y) + (x \leftrightarrow y), \quad (3.12)$$

for  $D = 6$ , and

$$K_A(x, y) = \frac{y}{x} \left(1 - \frac{4y}{5x} + \frac{y^2}{5x^2}\right) \theta(x - y) + (x \leftrightarrow y), \quad (3.13)$$

$$K_B(x, y) = \frac{1}{x} \left(1 - \frac{y}{2x} + \frac{y^2}{10x^2}\right) \theta(x - y) + (x \leftrightarrow y), \quad (3.14)$$

for  $D = 8$ . (See Appendix A for detail.)

Hereafter, we will use Landau gauge  $\xi = 0$  in which the wave function renormalization is absent ( $A(x) \equiv 1$ ) within the ladder approximation.

### 3.2 Improved ladder SD equation

It should be recalled here that we have so far neglected effects of the running of the gauge coupling. The power-like behavior of the running coupling makes its effects extremely important, however. In the analysis of D $\chi$ SB in four dimensional gauge theories, a widely used approximation is the so-called “improved” ladder approximation [16], in which the renormalization point  $\mu^2$  of the running coupling constant in the SD equation is replaced by  $\max(p_E^2, q_E^2)$ . This is a successful approximation for explaining properties of low energy QCD phenomenology. In the following analysis we adopt the improved ladder approximation and replace the gauge coupling  $g_D^2$  in Eq.(3.8) to

$$g_D^2 \rightarrow g_D^2(p_E, q_E) = \frac{\hat{g}^2(|p_E|)}{(p_E^2)^{\delta/2}} \theta(|p_E| - |q_E|) + \frac{\hat{g}^2(|q_E|)}{(q_E^2)^{\delta/2}} \theta(|q_E| - |p_E|). \quad (3.15)$$

As we have discussed in section 2, the UV fixed point  $g_*$  plays the role of the upper bound of  $\hat{g}$  in the ACDH scenario of the TMSM. We also note that the *dimensionless* bulk gauge coupling  $\hat{g}$  in Eq.(2.14) approaches very quickly to its fixed point for  $\mu > 1/R$  due to its power-law running and hence is *near the fixed point value over a wide*

range of the momentum in the integral of the SD equation. For the determination of the condition of the bulk D $\chi$ SB, it is therefore sufficient to investigate the SD equation with the coupling just on the UV fixed point:

$$B(x) = (D-1)\kappa_D \int_{M_0^2}^{\Lambda^2} dy y^{D/2-1} \frac{B(y)}{y + B^2(y)} K_B^{\text{imp}}(x, y) \quad (3.16)$$

with

$$\kappa_D \equiv C_F g_*^2 \Omega_{\text{NDA}} = \frac{C_F}{\left(\frac{2}{D-4} + 1\right) \left[\frac{26-D}{6} C_G - \frac{\eta}{3} T_R N_f\right]}, \quad (3.17)$$

where we have used Eqs.(2.8) and (2.15), and  $K_B^{\text{imp}}$  is given by

$$K_B^{\text{imp}}(x, y) = \frac{1}{x^2} \left(1 - \frac{y}{3x}\right) \theta(x - y) + (x \leftrightarrow y), \quad \text{for } D = 6, \quad (3.18)$$

and

$$K_B^{\text{imp}}(x, y) = \frac{1}{x^3} \left(1 - \frac{y}{2x} + \frac{y^2}{10x^2}\right) \theta(x - y) + (x \leftrightarrow y), \quad \text{for } D = 8. \quad (3.19)$$

Since the extra dimensions are compactified below the scale  $1/R$ , we have introduced the infrared (IR) cutoff  $M_0$  in Eq.(3.16). However, *the bulk D $\chi$ SB becomes insensitive to  $M_0$  for large  $\Lambda$*  as we will show in the next section. It is to be noted that the resulting *improved ladder* SD equation with the *running* coupling in Eq.(3.16) is a *scale-invariant* form, similar to the ladder SD equation with the *constant* gauge coupling in four dimensions.

We note that in the improved ladder SD equation Eq.(3.16), the  $\kappa_D$  defined by Eq.(3.17) plays the role of a “coupling”. Actually, it can be shown that there exists critical  $\kappa_D$  above which D $\chi$ SB takes place for sufficiently large  $\Lambda$  in the bulk.

## 4 Analysis for the improved ladder SD equation

### 4.1 Numerical study

The aim of this section is to determine the critical  $\kappa_D$  (and the scaling behavior around  $\kappa_D^{\text{crit}}$ ) by solving the SD equation Eq.(3.16) in a numerical method.

Let us start with the case  $D = 6$  and consider a discretized version of Eq.(3.16):

$$B_i = 5\kappa_6 \left[ \sum_{j=1}^i \frac{x_j B_j}{x_j + B_j^2} \frac{x_j^2}{x_i^2} \left(1 - \frac{x_j}{3x_i}\right) + \sum_{j=i+1}^{i_\Lambda} \frac{x_j B_j}{x_j + B_j^2} \left(1 - \frac{x_i}{3x_j}\right) \right] \quad (4.1)$$

with  $i, j$  being integer indices and

$$x_j \equiv M_0^2 \exp \left[ \frac{j-1}{i_\Lambda - 1} \ln \frac{\Lambda^2}{M_0^2} \right], \quad B_j \equiv B(x_j). \quad (4.2)$$

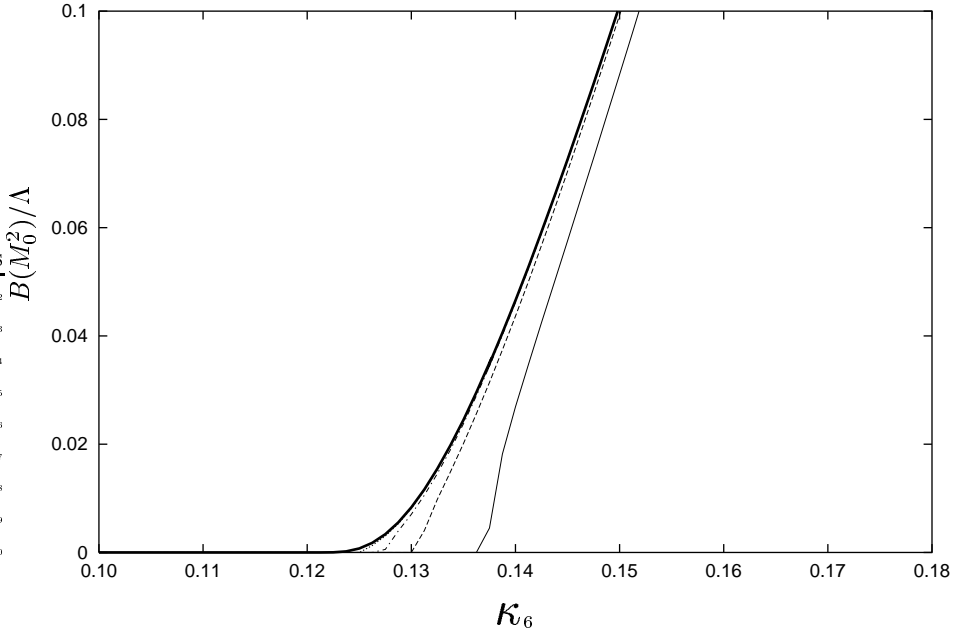


Figure 2: The scaling behavior in 6 dimensions. The lines from right to left are graphs for  $\Lambda^2/M_0^2 = 10^3, 10^4, 10^5, 10^6, 10^{10}$ , respectively.

In order to solve the discretized SD equation Eq.(4.1), a series  $B_j^{(n)}$  is defined by a recursion relation,

$$B_i^{(n+1)} \equiv 5\kappa_6 \left[ \sum_{j=1}^i \frac{x_j B_j^{(n)}}{x_j + (B_j^{(n)})^2} \frac{x_j^2}{x_i^2} \left(1 - \frac{x_j}{3x_i}\right) + \sum_{j=i+1}^{i_\Lambda} \frac{x_j B_j^{(n)}}{x_j + (B_j^{(n)})^2} \left(1 - \frac{x_i}{3x_j}\right) \right] \quad (4.3)$$

and an initial condition

$$B_j^{(n=0)} = M_0, \quad \text{for } j = 1, 2, \dots, i_\Lambda. \quad (4.4)$$

For sufficiently large  $n$ , the series  $B_j^{(n)}$  is numerically shown to converge to a certain  $B_j$ , which is nothing but the solution of the SD equation Eq.(4.1). It is also confirmed that the solution is insensitive to the value of  $i_\Lambda$ , if  $i_\Lambda$  is taken to be large enough.

Fig.2 shows the scaling behavior of the order parameter of D $\chi$ SB,  $B(M_0) = B_{j=1}$ , near the critical  $\kappa_6$ . We find

$$\kappa_6^{\text{crit}} \simeq 0.122. \quad (4.5)$$

On the other hand, the  $\kappa_6$  of the ACDH scenario with  $D = 6$  (QCD with 2 flavor fermion in the bulk) can be calculated from Eq.(3.17). We find

$$\kappa_6^{\text{ACDH}} = \frac{1}{11} \simeq 0.091, \quad (4.6)$$

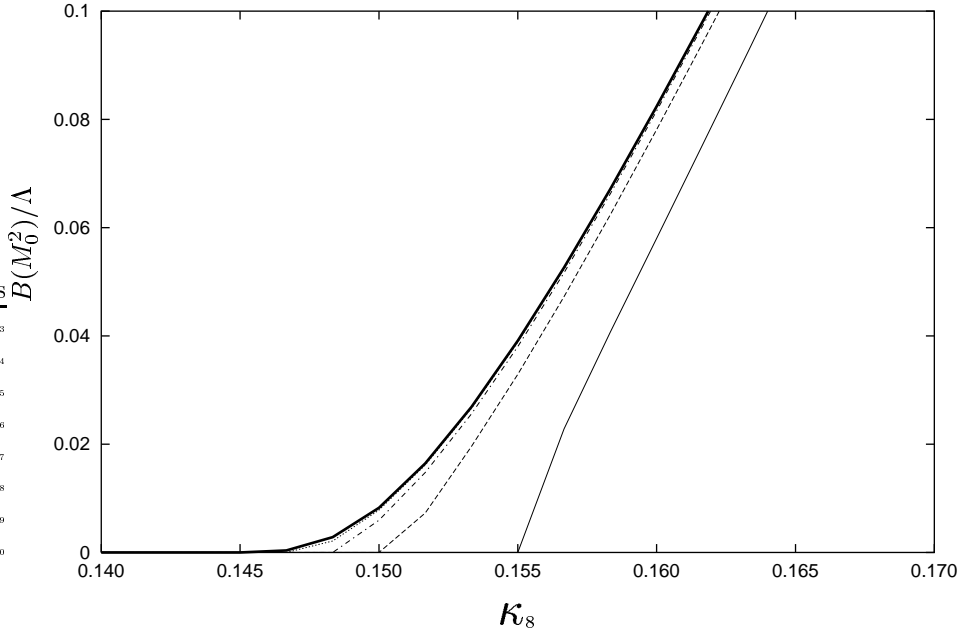


Figure 3: The scaling behavior in 8 dimensions. The lines from right to left are graphs for  $\Lambda^2/M_0^2 = 10^3, 10^4, 10^5, 10^6, 10^{10}$ , respectively.

where we have used  $C_F = 4/3$ ,  $C_G = 3$ ,  $N_f = 2$  and  $\eta = 8$ . Note that this is the *upper bound* of the bulk QCD coupling. We therefore conclude that the simplest version of the ACDH scenario does not work properly in  $D = 6$  dimensions within the improved ladder approximation.

Similar analysis is also performed for  $D = 8$  dimensions. We obtain the scaling behavior Fig.3, and the critical  $\kappa_8$ ,

$$\kappa_8^{\text{crit}} \simeq 0.146. \quad (4.7)$$

Since the ACDH scenario in  $D = 8$  dimensions predicts

$$\kappa_8^{\text{ACDH}} = \frac{8}{33} \simeq 0.242, \quad (4.8)$$

there is a possibility to construct viable models in  $D = 8$  within the improved ladder approximation.

One may doubt the validity of the ladder approximation in this model. The size of non-ladder corrections is estimated to be 1%–20% in the analysis of the four dimensional walking technicolor[28]. We expect similar size of non-ladder corrections in the present model. On the other hand, the fixed point Eq.(4.6) is smaller than the critical value Eq.(4.5) by more than 25%. Although it is extremely difficult to draw a definite conclusion from these numbers, it is likely that the ACDH scenario in  $D = 6$

dimensions is still in the chiral symmetric phase even in beyond-the-ladder approximations. We also note that the ladder results are qualitatively consistent with the naive dimensional analysis described in the section 2. The bulk QCD coupling is not so strong as to destroy the perturbative picture completely, anyway. We thus expect that our results (Fig.2 and Fig.3) are unchanged qualitatively even beyond-the-ladder approximation.

## 4.2 Analytical study

The improved ladder SD equation can be investigated analytically by applying further approximations. The SD equation can be greatly simplified if the integral kernel  $K_B^{\text{imp}}$  is approximated by

$$\tilde{K}_B^{\text{imp}}(x, y) = \frac{1}{x^{D/2-1}} \theta(x - y) + (x \leftrightarrow y). \quad (4.9)$$

The approximation Eq.(4.9) can be justified in a wide range of the integral region ( $x \not\simeq y$ ) in Eq.(3.16). We also note that the kernel Eq.(4.9) enjoys the scale invariance like the original kernel  $K_B^{\text{imp}}$ .

Although the SD equation Eq.(3.16) is still non-linear even under this approximation, we can overcome the difficulty by using the bifurcation technique [29], in which the mass function  $B$  in the denominator in the SD equation is eliminated and an infrared cutoff  $M \equiv B(M^2)$  is introduced instead. The bifurcation technique is justified when  $\kappa_D$  is close to its critical point.

The SD equation Eq.(3.16) then leads to a linear equation

$$B(x) = (D - 1)\kappa_D \int_{M^2}^{\Lambda^2} dy y^{D/2-2} B(y) \tilde{K}_B^{\text{imp}}(x, y), \quad (4.10)$$

and a subsidiary condition

$$M = B(M^2). \quad (4.11)$$

The integral equation Eq.(4.10) is equivalent to a set of a differential equation

$$\left[ x^2 \frac{d^2}{dx^2} + \frac{D}{2} x \frac{d}{dx} + (D - 1)(D/2 - 1)\kappa_D \right] B(x) = 0, \quad (4.12)$$

and boundary conditions

$$\left. \frac{d}{dx} B(x) \right|_{x=M^2} = 0, \quad (\text{IR-BC}) \quad (4.13)$$

$$\left. \left[ x \frac{d}{dx} - 2\omega \right] B(x) \right|_{x=\Lambda^2} = 0, \quad (\text{UV-BC}) \quad (4.14)$$

with  $\omega$  being defined by

$$\omega \equiv -\frac{1}{2} \left( \frac{D}{2} - 1 \right). \quad (4.15)$$

It is easy to solve the differential equation Eq.(4.12). Combined with the subsidiary condition Eq.(4.11) and the infrared boundary condition (IR-BC), we find

$$\frac{B(x)}{M} = \frac{1}{2\tilde{\nu}} \left( \frac{x}{M^2} \right)^\omega \left[ (1 + \tilde{\nu}) \left( \frac{x}{M^2} \right)^{-\omega\tilde{\nu}} - (1 - \tilde{\nu}) \left( \frac{x}{M^2} \right)^{\omega\tilde{\nu}} \right], \quad \tilde{\nu} \equiv \sqrt{1 - \kappa_D/\kappa_D^{\text{crit}}}, \quad (4.16)$$

for  $\kappa_D < \kappa_D^{\text{crit}}$  and

$$\frac{B(x)}{M} = \frac{1}{2i\nu} \left( \frac{x}{M^2} \right)^\omega \left[ (1 + i\nu) \left( \frac{x}{M^2} \right)^{-i\omega\nu} - (1 - i\nu) \left( \frac{x}{M^2} \right)^{i\omega\nu} \right], \quad \nu \equiv \sqrt{\kappa_D/\kappa_D^{\text{crit}} - 1}, \quad (4.17)$$

for  $\kappa_D > \kappa_D^{\text{crit}}$ , where we find the critical  $\kappa_D$ :

$$\kappa_D^{\text{crit}} \equiv \frac{1}{8} \frac{D-2}{D-1}. \quad (4.18)$$

Actually, the non-oscillating solution Eq.(4.16) for  $\kappa_D < \kappa_D^{\text{crit}}$  does not satisfy the ultraviolet boundary condition (UV-BC). Non-trivial solution of Eq.(4.10) exists only for  $\kappa_D > \kappa_D^{\text{crit}}$ , where the solution Eq.(4.17) starts oscillating. The critical  $\kappa_D$ , Eq.(4.18) reads  $\kappa_6^{\text{crit}} = 1/10$  and  $\kappa_8^{\text{crit}} = 3/28$ , which are slightly smaller than the numerical results in the previous section, Eq.(4.5) and Eq.(4.7). Noting the inequality of the integral kernels  $K_B^{\text{imp}} < \tilde{K}_B^{\text{imp}}$ , however, these results are consistent with each other.

We next turn to the scaling behavior near the critical point. Eq.(4.17) can be rewritten as

$$\frac{B(x)}{M} = \frac{\sqrt{1+\nu^2}}{\nu} \left( \frac{x}{M^2} \right)^\omega \sin \left[ \theta - \omega\nu \ln \frac{x}{M^2} \right], \quad e^{i\theta} \equiv \frac{1+i\nu}{\sqrt{1+\nu^2}}. \quad (4.19)$$

Plugging Eq.(4.19) into the UV-BC Eq.(4.14), we obtain

$$\theta - \omega\nu \ln \frac{\Lambda^2}{M^2} + \tan^{-1} \nu = n\pi, \quad (4.20)$$

with  $n$  being a positive integer. It can be shown that the ground state corresponds to the zero-node ( $n = 1$ ) solution [30]. Noting  $\theta = \tan^{-1} \nu \simeq \nu$  for  $\nu \ll 1$ , we thus obtain the scaling relation near the critical point

$$M \propto \Lambda \exp \left[ \frac{-\pi}{(D/2-1)\sqrt{\kappa_D/\kappa_D^{\text{crit}} - 1}} \right]. \quad (4.21)$$

Thus we found that the scaling of the phase transition Eq.(4.21) is an essential-singularity type, the ‘‘conformal phase transition’’ [17], similar to the result of the quenched ladder SD equation of the four dimensional QED [18]. It is suggestive that as we noted in the end of Section 3, these SD equations are both scale-invariant.

It is also worth pointing out that the essential singularity may be used to construct models with large hierarchy between the cutoff and the weak scale without introducing additional fine tuning. This important property of our analysis is contrasted to the NJL approach [7], where we need fine tuning of the NJL coupling strength with  $(M/\Lambda)^2$  level. (See Appendix B in detail.)

Near the critical point ( $\nu \rightarrow 0$  limit), Eq.(4.19) gives

$$B(x) = M \left( \frac{x}{M^2} \right)^{-(D/2-1)/2} \left( 1 + \frac{1}{2} \left( \frac{D}{2} - 1 \right) \ln \frac{x}{M^2} \right), \quad (4.22)$$

which is regarded as the asymptotic behavior of the solution of the SD equation Eq.(3.16).

## 5 Anomalous dimension of the fermion mass

We next consider generally the high energy behavior of the dynamical mass when the  $D\chi$ SB takes place, based on the OPE [31].

The OPE of the time-ordered fermion bilinear operator  $T[\psi(x)\bar{\psi}(0)]$  is given by

$$-i \int d^D x e^{iq \cdot x} T[\psi_i^a(x)\bar{\psi}_b^j(0)] = c_1^M(q, g_D; \mu) (\Gamma_M)_i^j \delta^a_b + c_{\bar{\psi}\psi}(q, g_D; \mu) \delta_i^j \delta^a_b (\bar{\psi}\psi) + \dots, \quad (5.1)$$

with  $c_1, c_{\bar{\psi}\psi}$  being the Wilson coefficient functions, where the suffices  $a, b$  are for gauge indices, and  $i, j$  are for spinor indices.

It is straightforward to evaluate the Wilson coefficient function  $c_{\bar{\psi}\psi}$  in the  $D = 4 + \delta$  dimensional gauge theories at the tree level,

$$c_{\bar{\psi}\psi}(q, \hat{g}; \mu) = \frac{(D-1)}{\eta} \frac{C_F}{N} \frac{\hat{g}^2}{\mu^\delta} \frac{1}{q^4}, \quad (5.2)$$

where we adopted the Landau gauge.

Comparing Eq.(5.1) with the propagator of the fermion field

$$-iS(p) = \frac{1}{A(-p^2)\not{p} - B(-p^2)} \simeq \frac{\not{p}}{A(-p^2)p^2} + \frac{B(-p^2)}{A^2(-p^2)p^2} + \dots, \quad (5.3)$$

we find that the high energy behavior of the dynamical fermion mass function  $B(-p^2)$  is given by

$$B(-p^2) \simeq p^2 c_{\bar{\psi}\psi}(p, \hat{g}; \mu) \langle \bar{\psi}\psi \rangle, \quad (5.4)$$

where we have assumed absence of the wave-function renormalization of the fermion field, which is justified in the Landau gauge within the ladder approximation.

The solution of RGE for  $c_{\bar{\psi}\psi}$  is given by,

$$\left[ \frac{\partial}{\partial t} - \hat{\beta} \frac{\partial}{\partial \hat{g}} + D - \gamma_m(\hat{g}) \right] c_{\bar{\psi}\psi}(e^t p, \hat{g}; \mu) = 0, \quad (5.5)$$

which is solved as

$$c_{\bar{\psi}\psi}(e^t p, \hat{g}; \mu) = c_{\bar{\psi}\psi}(p, \bar{g}(t); \mu) \exp \int_0^t dt [\gamma_m(\bar{g}(t)) - D], \quad (5.6)$$

with the running gauge coupling  $\bar{g}(t)$ :

$$\bar{g}^2(t) = \frac{1}{\frac{e^{-\delta t}}{\hat{g}^2(\mu)} - \left( \frac{2}{\delta} + 1 \right) \Omega_{\text{NDA}} b \left[ 1 - e^{-\delta t} \right]}. \quad (5.7)$$

For sufficiently large  $t$ , it is evident that  $\lim_{t \rightarrow \infty} \bar{g}(t) = g_*$ . The high energy behavior of the Wilson coefficient function  $c_{\bar{\psi}\psi}$  therefore reads

$$c_{\bar{\psi}\psi}(e^t p, \hat{g}; \mu) \propto e^{(\gamma_m^* - D)t}, \quad \gamma_m^* \equiv \gamma_m(g_*) \quad (5.8)$$

or

$$c_{\bar{\psi}\psi}(p, \hat{g}; \mu) \propto (-p^2)^{(\gamma_m^* - D)/2}. \quad (5.9)$$

The high energy behavior of the mass function  $B$  in Eq.(5.4) thus is given by

$$B(-p^2) \propto (-p^2)^{(\gamma_m^* + 2 - D)/2}. \quad (5.10)$$

The anomalous dimension at the fixed point  $\gamma_m^*$  can be extracted from the numerical solution of the SD equation. For such a purpose we define the “power” of the mass function ( $\omega$ )

$$\omega \equiv \frac{x}{B(x)} \frac{d}{dx} B(x). \quad (5.11)$$

Fig.4 shows the “power” behaviors of the numerical solution of the SD equation in six dimensions for various “couplings”. It can be seen that the “power” is almost constant in the asymptotic region  $B^2(M_0) \ll x \ll \Lambda^2$  as we expected from Eq.(5.10). The behavior near the cutoff  $x \simeq \Lambda^2$  in Fig. 4 is an artifact [32] due to the sharp cutoff introduced in the analysis of the SD equation<sup>4</sup>. This artifact disappears at the limit of  $\Lambda \rightarrow \infty$ . Reading the “power” in the asymptotic region ( $\omega \simeq -1$ ), we obtain

$$\gamma_m^* \simeq 2\omega + (D - 2) \simeq 2 \quad (5.12)$$

---

<sup>4</sup> Eq.(4.14) leads to the relation of  $\Lambda^2 B'(\Lambda^2)/B(\Lambda^2) = 1 - D/2$ .

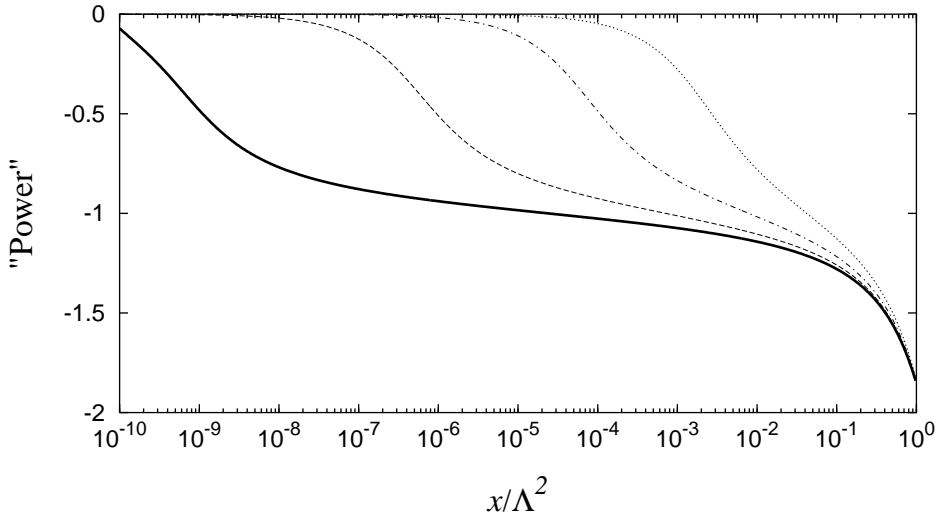


Figure 4: The “power” behavior of the mass function in 6 dimensions. The lines from left to right represent graphs for  $\kappa_6 = 0.122, 0.125, 0.130, 0.140$  (or  $B^2(M_0^2)/\Lambda^2 = 4.1 \times 10^{-10}, 5.4 \times 10^{-7}, 6.9 \times 10^{-5}, 2.2 \times 10^{-3}$ ) with  $\Lambda^2/M_0^2 = 10^{10}$ .

for the  $D = 6$  bulk gauge theory at the critical point  $\kappa_6^{\text{crit}}$ .

Similar analysis is also performed for  $D = 8$ . The corresponding “power” behavior is shown in Fig.5. The anomalous dimension is then

$$\gamma_m^* \simeq 2\omega + (D - 2) \simeq 3, \quad (5.13)$$

for  $D = 8$ .

On the other hand, the analytical result in the previous section Eq.(4.22) compared with Eq.(5.10) yields

$$\gamma_m^* = \frac{D}{2} - 1, \quad (5.14)$$

which agrees with the above numerical one.

It is remarkable that Eq.(5.14) is also consistent with the conformal phase transitions for other dimensions  $D \leq 4$ :  $\gamma_m = 1/2$  for  $D = 3$  agrees with the high energy behavior [33] and  $\gamma_m = 1$  for  $D = 4$  is the walking theory [19] obtained from the ladder SD equation with fixed coupling. They are obtained in different approximations: Namely, the result of three dimensions is by the running coupling with the IR-fixed point and that of six/eight dimensions is by the running coupling with the UV fixed point, while the four dimensional result is by the fixed coupling. However, the SD equations in all these cases happen to be quite similar because of the *scale invariance at the fixed point*.

It should be emphasized that such a large anomalous dimension implies suppression of the flavor-changing-neutral-current (FCNC) problem in the dynamical electroweak symmetry breaking scenario as in walking technicolor [19]. The large  $\gamma_m$  observed in

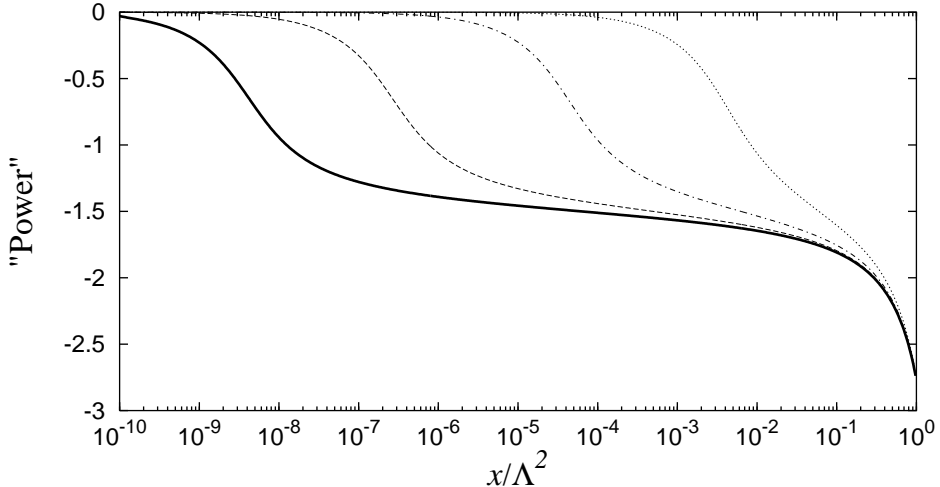


Figure 5: The “power” behavior of the mass function in 8 dimensions. The lines from left to right represent graphs for  $\kappa_8 = 0.146, 0.147, 0.150, 0.160$  (or  $B^2(M_0^2)/\Lambda^2 = 5.8 \times 10^{-9}, 4.1 \times 10^{-7}, 6.8 \times 10^{-5}, 6.8 \times 10^{-3}$ ) with  $\Lambda^2/M_0^2 = 10^{10}$ .

this section is, therefore, a good news to construct phenomenologically viable models in this direction.

Moreover, the corresponding asymptotic behavior of the mass function Eq.(4.22),  $B(p_E^2) \sim M^{D/2}(p_E^2)^{(1-D/2)/2}$ , still yields strong convergence of the bulk decay constant  $F_\pi^{(D)}$  which may be calculated through the PS formula [4]:

$$(F_\pi^{(D)})^2 \sim \int \frac{d^D p_E}{(2\pi)^D} \frac{B^2(p_E^2)}{(p_E^2 + B^2(p_E^2))^2},$$

$$\propto M^D \int dp_E \frac{1}{p_E^3}. \quad (5.15)$$

Then it suggests that the dynamically induced bulk Yukawa coupling  $g_Y = M/F_\pi^{(D)}$  can be made finite even in the “infinite cutoff limit”  $\Lambda \rightarrow \infty$ .<sup>5</sup> This is contrasted to the perturbation theory where the gauge theory in  $D(> 4)$  dimensions is obviously non-renormalizable. This situation is similar to the renormalizability of the gauged NJL model [20].

## 6 Chiral fermion on the 3-brane

We have investigated so far the possibility of D $\chi$ SB in the bulk. Since a chiral fermion in the bulk ( $D > 4$ ) has four or larger number of components, it is non-trivial to

<sup>5</sup>This statement is of course rather formal in the sense that  $\kappa_D$  in Eq.(3.17) is actually not an arbitrary adjustable parameter and hence cannot be fine-tuned to  $\kappa_D^{\text{crit}}$ ,  $\kappa_D \rightarrow \kappa_D^{\text{crit}}$ , to make the dynamical mass  $M$  to be finite through Eq.(4.21) in that limit.

obtain a four dimensional chiral fermion with two components as an effective theory. For such a purpose, we need to compactify the extra dimensions on an orbifold, in which unwanted components are projected out by its boundary conditions [7]. In this section we describe a systematic procedure to find such orbifold compactifications.

We start with the minimal case,  $D = 6$  for simplicity. The chiral projection operators in six dimensions are given by

$$\frac{1 \pm \Gamma_{A,7}}{2}, \quad \Gamma_{A,7} \equiv \Gamma^0 \Gamma^1 \Gamma^2 \Gamma^3 \Gamma^5 \Gamma^6, \quad (6.1)$$

and the chiral fermions  $\psi_{\pm}$  obey

$$\Gamma_{A,7} \psi_{\pm} = \pm \psi_{\pm}. \quad (6.2)$$

Hereafter we argue only  $\psi_+$ , the chiral fermion with positive chirality in the bulk. It is easy to extend our arguments to the case of  $\psi_-$ .

We next decompose the space-time coordinate into conventional and extra dimensions:

$$x^M = (x^\mu, y^m), \quad \mu = 0, 1, 2, 3, \quad m = 5, 6, \quad (6.3)$$

and assume a torus compactification,

$$\psi_+(x, y^5, y^6) = \psi_+(x, y^5 + 2\pi R, y^6) = \psi_+(x, y^5, y^6 + 2\pi R), \quad (6.4)$$

where radii of the fifth and sixth dimensions are assumed to be the same (denoted by  $R$ ) for simplicity. The chiral fermion in  $D = 6$  is then decomposed into KK modes:

$$\psi_+(x, y) = \sum_{k_5, k_6} \psi_+^{k_5 k_6}(x) \exp \left[ i \frac{k_5 y^5 + k_6 y^6}{R} \right]. \quad (6.5)$$

We next introduce four-dimensional chirality matrix  $\Gamma_{A,5} \equiv i \Gamma^0 \Gamma^1 \Gamma^2 \Gamma^3$ . It is easy to show several identities

$$[\Gamma_{A,5}, \Gamma_{A,7}] = 0, \quad \Gamma_{A,5} \Gamma_{A,5} = 1, \quad \text{tr} \left[ \Gamma_{A,5} \frac{1 \pm \Gamma_{A,7}}{2} \right] = 0, \quad (6.6)$$

which indicate that  $\Gamma_{A,5}$  and  $\Gamma_{A,7}$  are simultaneously diagonalizable, eigenvalues of  $\Gamma_{A,5}$  are  $\pm 1$ , and that the sum of eigenvalues of  $\Gamma_{A,5}$  is zero for a chiral fermion in the six dimensional bulk. It is therefore evident that the zero mode  $\psi_+^{00}$  in this torus compactification is vector-like in its four dimensional effective theory. We need to eliminate unwanted components of the fermion on the four dimensional brane by imposing certain orbifold symmetry.

It should be noted, however, that the “parity” of extra dimensions does not suit our purpose, because it is explicitly violated in the chiral theory of the bulk.<sup>6</sup> We then

---

<sup>6</sup>  $CP$  is also violated in the six dimensional bulk, since the charge conjugation does not flip chirality in  $D = 4k + 2$  dimensions.

try to adopt the rotation in the extra dimensions with angle  $\pi$ :<sup>7</sup>

$$\begin{aligned}\psi'(x, y^5, y^6) &= \exp\left[\frac{i}{2}\Sigma^{56}\pi\right]\psi(x, -y^5, -y^6) \\ &= i\Sigma^{56}\psi(x, -y^5, -y^6),\end{aligned}\quad (6.7)$$

with  $\Sigma^{MN}$  being defined by

$$\Sigma^{MN} \equiv \frac{i}{2}[\Gamma^M, \Gamma^N]. \quad (6.8)$$

There are two possible boundary conditions of this orbifold:

$$\psi_+(x, y^5, y^6) = (-1)^n \Sigma^{56} \psi_+(x, -y^5, -y^6), \quad n = 0 \text{ or } 1, \quad (6.9)$$

which leads to a constraint for the zero mode fermion

$$\psi_+^{00}(x) = (-1)^n \Sigma^{56} \psi_+^{00}(x). \quad (6.10)$$

Noting an identity  $\Sigma^{56} = -\Gamma_{A,5}\Gamma_{A,7}$ , we can rewrite Eq.(6.10) into the conditions of the chiral fermion on the four dimensional brane:

$$\Gamma_{A,5}\psi_+^{00}(x) = (-1)^{n+1} \psi_+^{00}(x). \quad (6.11)$$

The chirality on the brane is determined depending on the choice of the boundary condition,  $n = 0$  or  $1$ , in Eq.(6.9)

It should be emphasized here that our procedures described in this section do not depend on a particular choice of the representation of the Clifford algebra. We can easily generalize our arguments to an orbifold compactification from  $D = 2(k+1)$  into  $D = 2k$  dimensions. By applying these procedures repeatedly, we are thus able to obtain orbifold compactification starting from a bulk chiral theory of  $D = 2k$  ( $k \geq 3$ ) into a brane chiral theory with four dimensions.

## 7 Effective gauge coupling

Although the  $\overline{MS}$ -scheme has been widely adopted for the running gauge coupling in the improved ladder approximation, it would be worth investigating yet another choice, “effective” gauge coupling  $g_{\text{eff}}$ , which is closely related to the gauge boson propagator and its momentum.

For such a purpose, we evaluate the one-loop gauge boson propagator in the truncated KK effective theory on the 3-brane, and derive a relation between the effective and the  $\overline{MS}$  couplings.

---

<sup>7</sup> It is also possible to use  $\pi/2$  rotation to define an orbifold which keeps chirality on the four-dimensional brane.

The effective gauge coupling  $g_{\text{eff}}$  on the 3-brane is defined by:<sup>8</sup>

$$\frac{-i}{g_{\text{eff}}^2(q^2)} D_{\mu\nu}^{-1}(q) \equiv \frac{-i}{g_0^2} D_{(0)\mu\nu}^{-1}(q) - (q^2 g_{\mu\nu} - q_\mu q_\nu) \Pi(q^2), \quad (7.1)$$

with  $g_0$  being bare gauge coupling and the (four-dimensional) gauge boson propagators are given by

$$D_{(0)\mu\nu}(q) = \frac{-i}{q^2} \left( g_{\mu\nu} - (1 - \xi_0) \frac{q_\mu q_\nu}{q^2} \right), \quad D_{\mu\nu}(q) = \frac{-i}{q^2} \left( g_{\mu\nu} - (1 - \xi_{\text{eff}}(q^2)) \frac{q_\mu q_\nu}{q^2} \right). \quad (7.2)$$

Eq.(7.1) reads

$$\frac{1}{g_{\text{eff}}^2(q^2)} = \frac{1}{g_0^2} - \Pi(q^2). \quad (7.3)$$

The vacuum polarization function  $\Pi(q^2)$  can be decomposed into loops of each KK modes at the one-loop level:

$$\Pi(q^2) = \sum_{\vec{n}} \Pi(q^2, m_{\vec{n}}^2), \quad m_{\vec{n}}^2 = \frac{|\vec{n}|^2}{R^2}. \quad (7.4)$$

In order to calculate the relation between the effective and the  $\overline{MS}$  couplings, we next evaluate  $\Pi(q^2, m_{\vec{n}}^2)$  using the dimensional regularization ( $d \equiv 4 + \epsilon$ ):

$$\Pi(q^2, m^2) = C_G \left[ 4I_g(q^2, m^2) + (2 - D)I_b(q^2, m^2) \right] - 2\eta T_R N_f I_f(q^2, m^2), \quad (7.5)$$

where we used notations introduced in section 2 and

$$\begin{aligned} I_g(q^2, m^2) &\equiv \frac{\Gamma(2 - d/2)}{(4\pi)^{d/2}} \int_0^1 dx \left[ m^2 - x(1 - x)q^2 \right]^{d/2-2}, \\ I_b(q^2, m^2) &\equiv \frac{\Gamma(2 - d/2)}{2(4\pi)^{d/2}} \int_0^1 dx (2x - 1)^2 \left[ m^2 - x(1 - x)q^2 \right]^{d/2-2}, \\ I_f(q^2, m^2) &\equiv \frac{\Gamma(2 - d/2)}{(4\pi)^{d/2}} \int_0^1 dx x(1 - x) \left[ m^2 - x(1 - x)q^2 \right]^{d/2-2}. \end{aligned}$$

The counter term for the  $\overline{MS}$  coupling<sup>9</sup> in the truncated KK effective theory is given by

$$\frac{1}{g_{\overline{MS}}^2(\mu)} = \frac{1}{g_0^2} - \sum_{\vec{n}}^{m_{\vec{n}} > \mu} \Pi(q^2 = 0, m_{\vec{n}}^2) + \sum_{\vec{n}}^{m_{\vec{n}} \leq \mu} \frac{\Gamma(2 - d/2)}{(4\pi)^{d/2}} b' \mu^{d-4}, \quad (7.6)$$

<sup>8</sup> We use the background gauge fixing method throughout in this section. The Ward-Takahashi identities of non-Abelian gauge theory are QED-like and keep manifest gauge invariance in this gauge fixing.

<sup>9</sup> Strictly speaking, Eq.(7.6) is evaluated in the modified dimensional reduction scheme [34].

where the term  $\sum_{\vec{n}}^{m_{\vec{n}} > \mu} \Pi(q^2 = 0, m_{\vec{n}}^2)$  comes from the loop of KK-modes heavier than the renormalization scale  $\mu$ . This term is independent of  $\mu$  and therefore does not affect the RGE for the gauge coupling, in accordance with the decoupling theorem which is assumed in the truncated KK effective theory.

Taking  $d \rightarrow 4$  limit we now obtain

$$\frac{1}{g_{\text{eff}}^2(q^2)} = \frac{1}{g_{\overline{MS}}^2(\mu)} - \sum_{\vec{n}}^{m_{\vec{n}} > \mu} \Pi_{>}(q^2, m_{\vec{n}}^2) - \sum_{\vec{n}}^{m_{\vec{n}} \leq \mu} \Pi_{<}(q^2, m_{\vec{n}}^2; \mu), \quad (7.7)$$

where  $\Pi_{>}$  and  $\Pi_{<}$  are given by

$$\begin{aligned} (4\pi)^2 \Pi_{>}(q^2, m^2) &\equiv -C_G \int_0^1 dx \left[ 4 + \frac{2-D}{2}(2x-1)^2 \right] \ln \left( 1 - \frac{q^2}{m^2} x(1-x) \right) \\ &\quad + 2\eta T_R N_f \int_0^1 dx x(1-x) \ln \left( 1 - \frac{q^2}{m^2} x(1-x) \right), \end{aligned} \quad (7.8)$$

$$\begin{aligned} (4\pi)^2 \Pi_{<}(q^2, m^2; \mu) &\equiv -C_G \int_0^1 dx \left[ 4 + \frac{2-D}{2}(2x-1)^2 \right] \ln \left( \frac{m^2 - q^2 x(1-x)}{\mu^2} \right) \\ &\quad + 2\eta T_R N_f \int_0^1 dx x(1-x) \ln \left( \frac{m^2 - q^2 x(1-x)}{\mu^2} \right). \end{aligned} \quad (7.9)$$

Note here that the  $\mu$  dependence in the RHS of (7.7) cancels exactly. We also introduce a *dimensionless* effective gauge coupling of the *bulk* gauge theory defined in a similar manner to Eq.(2.2),

$$\hat{g}_{\text{eff}}^2(q^2) = \frac{(2\pi R \sqrt{-q^2})^\delta}{n} g_{\text{eff}}^2(q^2). \quad (7.10)$$

Using approximations described in Appendix C, we find

$$\frac{1}{\hat{g}_{\text{eff}}^2(q^2)} \simeq \frac{\lambda}{\hat{g}_{\overline{MS}}^2(\sqrt{-\lambda q^2})} + \frac{1}{(4\pi)^3} \left[ -\frac{3}{5} C_G + \frac{\eta}{15} T_R N_f \right] \ln \left( \frac{-\lambda q^2}{\Lambda^2} \right), \quad (7.11)$$

for the bulk gauge theory in  $D = 6$  dimensions. Here  $\lambda$  is given by

$$\lambda = \exp \left[ \frac{C_G \left( -8 - \frac{4}{9}(2-D) \right) + \frac{5}{9} \eta T_R N_f}{-b'} \right]. \quad (7.12)$$

In the analysis of the SD equation based on the  $g_{\text{eff}}$ , we adopt the effective coupling  $\hat{g}_{\text{eff}}^2$  Eq.(7.11) (instead of  $\hat{g}_{\overline{MS}}^2$  in Eq.(2.14)) in the formula of the improved ladder approximation Eq.(3.15).

Several comments are in order:

a) Decoupling theorem is violated in the effective coupling Eq.(7.11), since it depends

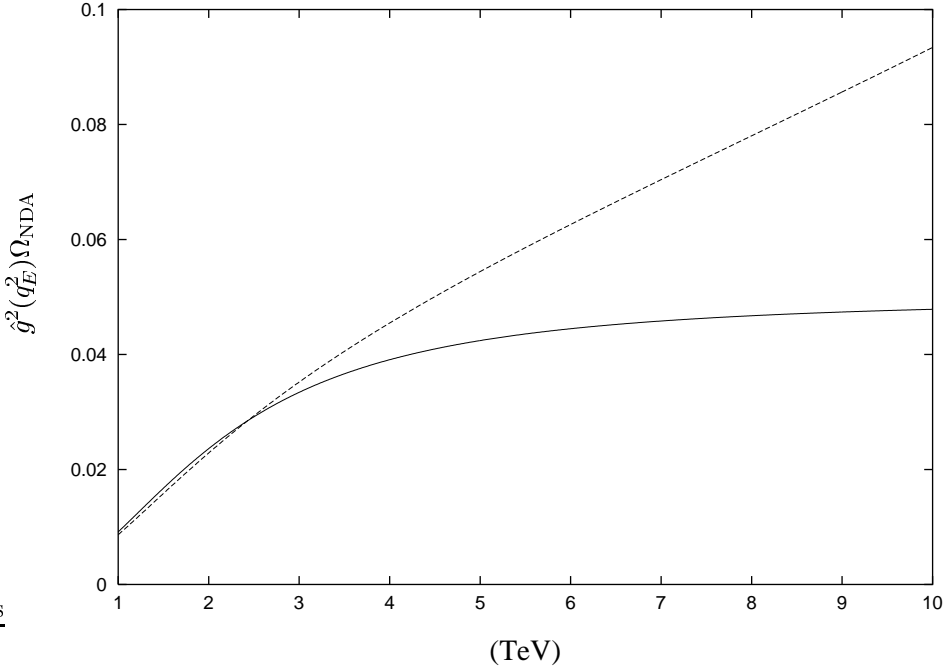


Figure 6: The graph of the dimensionless gauge coupling with  $C_G = 3$ ,  $N_f = 0$ ,  $R^{-1} = 1\text{TeV}$ ,  $\Lambda = 10\text{TeV}$ ,  $\alpha_{\overline{MS}}(M_Z) = 0.1$ . The solid line and the dashed line represent the  $\overline{MS}$  coupling and the effective coupling of Eq.(7.11), respectively.

explicitly on the ultraviolet cutoff  $\Lambda$ . This result comes from the non-renormalizability of the six dimensional bulk gauge theory.

- b) The effective coupling is larger than the  $\overline{MS}$  one approximately by factor  $\lambda^{-1}$ . (See also Fig.6). If we adopt  $\hat{g}_{\text{eff}}$  instead of  $\hat{g}_{\overline{MS}}$  in the improved ladder approximation, there is a chance that the bulk QCD coupling even in the six dimensions can be strong enough to cause D $\chi$ SB in the bulk under certain conditions.
- c) There still exists an *upper bound* on  $\hat{g}_{\text{eff}}$  similarly to the non-trivial UV fixed point, which is roughly proportional to the UV fixed point in the  $\overline{MS}$  scheme. (See Appendix C for detailed discussion.) It is therefore still non-trivial question whether D $\chi$ SB occurs or not in the bulk gauge theories even if we adopt  $\hat{g}_{\text{eff}}$  in the improved ladder SD equation.
- d) We can define an analogue of “ $\beta$ -function” for “bare coupling”  $\hat{g}_\Lambda \equiv \hat{g}_{\text{eff}}(q^2 = -\Lambda^2)$ . (See Appendix C.) The upper bound of  $\hat{g}_{\text{eff}}$  can be regarded as a UV fixed point of such a “ $\beta$ -function” and therefore independent of the choice of the cutoff scale  $\Lambda$ .

Actually the finite renormalization effect is the largest uncertainty of our analysis based on the improved ladder SD equation, compared with other uncertainties such as the non-ladder effects, higher order corrections, etc.. The detailed analysis of the improved ladder SD equation with  $\hat{g}_{\text{eff}}$  will be presented elsewhere [35].

## 8 Summary and discussions

We have studied dynamical issues of the ACDH version [7] of the TMSM [1, 2, 3, 5] within the framework of the improved ladder SD equation. Based on the truncated KK effective theory [15], we found that the  $D$ -dimensional non-Abelian gauge theories with the compactified extra dimensions possess a non-trivial UV fixed point. We then evaluated the UV fixed point by using one-loop RGE, assuming its non-perturbative existence. Although the SM couplings in the  $D$ -dimensional bulk become generally strong beyond the compactification scale, the (dimensionless) bulk coupling cannot grow beyond the UV fixed point and hence it is highly non-trivial whether the  $D\chi$ SB really takes place or not.

For the simplest scenario of ACDH where the massless gauge bosons and third family quarks and leptons living in the  $D$ -dimensional bulk and the rest in the four-dimensional brane (3-brane), we have the UV fixed points Eqs.(4.6), (4.8):

$$\kappa_6 = 0.091, \quad \kappa_8 = 0.242 \quad (8.1)$$

for the bulk dimensions being six and eight, respectively.

On the other hand, the improved ladder SD equation in  $D(> 4)$  dimensions yields the critical points in six/eight dimensions as Eqs.(4.5), (4.7):

$$\kappa_6^{\text{crit}} = 0.122, \quad \kappa_8^{\text{crit}} = 0.146. \quad (8.2)$$

These results are qualitatively consistent with the naive dimensional analysis. The ACDH scenario thus can work for  $D = 8$  but not  $D = 6$  if we take the results Eq.(8.1) and Eq.(8.2) at face value. It should be emphasized, however, that our analysis is based on the ladder approximation. We would certainly need further investigation to incorporate non-ladder effects in order to evaluate the critical value more accurately.

We also discussed some subtlety about the “improving” ladder SD equation by replacing the  $\overline{MS}$  running by the effective coupling including the finite renormalization effects. This makes attractive forces somewhat larger than the  $\overline{MS}$  ones, so that the condensate can take place more easily. In the case of the ACDH scenario, the top condensation may be possible due to effects of finite renormalization even in six dimensions, since the coupling has a chance to grow over the critical point *for sufficiently large cutoff*.

On the other hand, if the cutoff is too large, then the  $U(1)$  coupling would dominate the QCD coupling so that the MAC favors other channel (tau lepton condensate) than the top quark condensate. We then obtain some conditions for the “effective (phenomenological) cutoff” ( $\Lambda$ ) where the bulk QCD and hypercharge couplings are aligned in the MAC in such a way that only the top quark condenses while others (bottom, etc.) do not. Another constraint will come from the top quark mass which is related to the decay constant  $F_\pi^{(D)}$  in  $D$  dimensions through the PS formula, Eq.(5.15). Then it is related to the weak scale  $F_\pi = 246\text{GeV}$  as

$$F_\pi^2 = \frac{(2\pi R)^\delta}{n} (F_\pi^{(D)})^2. \quad (8.3)$$

These matters will be dealt with in the forthcoming paper [35].

The salient feature of the improved ladder SD equation in  $D(> 4)$  dimensions is its approximate scale-invariance. The reason is the followings: The bulk dimensionful coupling can be written as the dimensionless coupling multiplied by a factor having dimensions carried by the renormalization point  $\mu$  (see Eq.(2.11)) which is then traded for the momentum in the running coupling in the improved ladder SD equation, and moreover the running coupling quickly grows up to the UV fixed point. Hence the SD equation can well be approximated by the coupling at the fixed point. Then the resultant SD equation Eq.(3.16) has no scale parameters except for the cutoff.

This is the very reason why we obtained the essential-singularity scaling of the conformal phase transition, Eq.(4.21), with the analytical result for the critical point Eq.(4.18):

$$\kappa_D^{\text{crit}} = \frac{D-2}{8(D-1)}, \quad (8.4)$$

which was derived through certain approximations and is consistent with the numerical result above.

The essential-singularity scaling gives us a possibility to have a large hierarchy between the weak scale and the cutoff without fine-tuning. Here we note that  $\kappa_D$  is not an arbitrary parameter but a definite number once the model is set up. We should therefore note that it is impossible to take the cutoff infinitely large.

In a realistic model building based on the ACDH scenario, however, the bulk gauge coupling of QCD is determined through the matching with the QCD on the 3-brane at the compactification scale  $R^{-1}$ . The bulk coupling grows in the high energy toward the UV fixed point and can exceed the critical coupling only for a certain cutoff (“critical cutoff”). When we tune the cutoff very close to the critical one, the SD equation yields a very small dynamical mass compared with the cutoff. We are thus able to determine the value of the cutoff, which enables us to evaluate the low energy predictions of the ACDH scenario (e.g.,  $m_t$  and  $m_H$ ) more accurately.

Moreover, we had a very large anomalous dimension Eq.(5.14):

$$\gamma_m = \frac{D}{2} - 1, \quad (8.5)$$

which happen to coincide with the cases for  $D \leq 4$ , i.e., the quenched ladder SD equation (with non-running or walking/standing coupling) for  $D = 4$  ( $\gamma_m = 1$ ) and also with the improved ladder SD equation for  $D = 3$  QED ( $\gamma_m = 1/2$ ) where the running coupling has an infrared fixed point. In all the cases including  $D \leq 4$ , the SD equation has a scale invariance at the fixed point.

## Acknowledgements

We would like to thank Howard Georgi, Valery Gusynin, Masayasu Harada, Yoshio Kikukawa, Volodya Miransky, Takeo Moroi, Masahiro Yamaguchi for useful discussions.

K. Y. thanks Howard Georgi for hospitality at Harvard where a part of this work was done. This work is supported by Grant-in-Aid for Scientific Research (B) #11695030 (K.Y.), (A) #12014206 (K.Y.), and JSPS Research Fellowships for Young Scientists #01170 (M.H.), and by the Oversea Research Scholar Program of the Monbusho (Ministry of Education, Science, Sports and Culture) (K.Y.).

## A Angular integrals in the ladder SD equations

The momentum integrals of the SD equations Eq.(3.5) and Eq.(3.6) can be decomposed into polar and angular integrals,

$$\int \frac{d^D q_E}{(2\pi)^D} F(p_E^2, q_E^2, p_E \cdot q_E) = C_D \int_0^{\Lambda^2} dy y^{D/2-1} \int_0^\pi d\theta \sin^{D-2} \theta F(x, y, \sqrt{xy} \cos \theta), \quad (\text{A.1})$$

with  $x \equiv p_E^2$ ,  $y \equiv q_E^2$  and  $C_D$  is defined by  $C_D \equiv \Omega_{\text{NDA}}/B(1/2, D/2 - 1/2)$ . In order to evaluate the angular integral  $d\theta$ , we define the integral,

$$I(\mu, \nu, \rho; z) \equiv \int_0^\pi d\theta \frac{\sin^{2\nu+1} \theta \cos^\rho \theta}{(z - \cos \theta)^{\mu+\nu+1}}. \quad (\text{A.2})$$

It is easy to see that the angular integrals in Eq.(3.5) and Eq.(3.6) can be expressed in terms of  $I(\mu, \nu, 0; z)$  and  $I(\mu, \nu, 1; z)$  with  $z \equiv (x + y)/(2\sqrt{xy})$ . We obtain [23]

$$\begin{aligned} A(x) &= 1 + \frac{C_F g_D^2}{x} C_D \int_0^{\Lambda^2} dy y^{D/2-1} \frac{A(y)}{A^2 y + B^2} \times \\ &\quad \times \left\{ \frac{D-1-\xi}{2} I\left(\frac{3}{2} - \frac{D}{2}, \frac{D}{2} - \frac{3}{2}, 1; z\right) - \frac{1-\xi}{2} I\left(\frac{3}{2} - \frac{D}{2}, \frac{D}{2} - \frac{1}{2}, 0; z\right) \right\} \quad (\text{A.3}) \\ B(x) &= (D-1+\xi) C_F g_D^2 C_D \int_0^{\Lambda^2} dy y^{D/2-1} \frac{B(y)}{A^2 y + B^2} \frac{1}{2\sqrt{xy}} I\left(\frac{3}{2} - \frac{D}{2}, \frac{D}{2} - \frac{3}{2}, 0; z\right). \end{aligned} \quad (\text{A.4})$$

Using a relation

$$I(\mu, \nu, 1; z) = \frac{1}{2\nu+2} \int_0^\pi d\theta \frac{1}{(z - \cos \theta)^{\mu+\nu+1}} \frac{d}{d\theta} [\sin^{2\nu+2} \theta] = \frac{\mu+\nu+1}{2\nu+2} I(\mu, \nu+1, 0; z), \quad (\text{A.5})$$

Eq.(A.3) can be further simplified

$$A(x) = 1 + \frac{\xi}{2} \frac{D-2}{D-1} \frac{C_F g_D^2}{x} C_D \int_0^{\Lambda^2} dy y^{D/2-1} \frac{A(y)}{A^2 y + B^2} I\left(\frac{3}{2} - \frac{D}{2}, \frac{D}{2} - \frac{1}{2}, 0; z\right). \quad (\text{A.6})$$

It should be noted that  $A(x) = 1$  holds for arbitrary dimensions in the Landau gauge  $\xi = 0$ . [23]

The integral  $I(\mu, \nu, 0; z)$  was given for certain integer dimensions in Ref. [23] and now is expressed in terms of the hypergeometric function  $F(\alpha, \beta, \gamma; z)$  for arbitrary  $D$ :

$$I(\mu, \nu, 0; z) = \frac{2^{\mu+\nu+1} \sqrt{\pi} \Gamma(\nu+1)}{\tilde{z}^{\mu+\nu+1} \Gamma(\nu + \frac{3}{2})} F(\mu + \nu + 1, \mu + \frac{1}{2}, \nu + \frac{3}{2}; \tilde{z}^{-2}), \quad (\text{A.7})$$

with

$$\tilde{z} \equiv z + \sqrt{z^2 - 1} = \frac{\max(x, y)}{\sqrt{xy}}, \quad \tilde{z}^{-2} = \frac{\min(x, y)}{\max(x, y)}. \quad (\text{A.8})$$

We thus obtain the integral kernel  $K_A$ ,

$$K_A(x, y) = \tilde{z}^{-2} F(2, 2 - D/2, D/2 + 1; \tilde{z}^{-2}), \quad (\text{A.9})$$

and the integral kernel  $K_B$  [36],

$$K_B(x, y) = \frac{1}{\max(x, y)} F(1, 2 - D/2, D/2; \tilde{z}^{-2}). \quad (\text{A.10})$$

Using the Taylor expansion of the hypergeometric function

$$F(\alpha, \beta, \gamma; z) = \sum_{\ell=0}^{\infty} \frac{(\alpha)_\ell (\beta)_\ell z^\ell}{(\gamma)_\ell \ell!}, \quad (\alpha)_\ell \equiv \alpha(\alpha+1)(\alpha+2) \cdots (\alpha+\ell-1),$$

we obtain

$$K_A(x, y) \equiv \frac{y}{x} \sum_{\ell=0}^{\delta/2} \frac{(-\delta/2)_\ell (\ell+1)}{(\delta/2+3)_\ell} \left(\frac{y}{x}\right)^\ell \theta(x-y) + (x \leftrightarrow y), \quad (\text{A.11})$$

$$K_B(x, y) \equiv \frac{1}{x} \sum_{\ell=0}^{\delta/2} \frac{(-\delta/2)_\ell}{(\delta/2+2)_\ell} \left(\frac{y}{x}\right)^\ell \theta(x-y) + (x \leftrightarrow y), \quad (\text{A.12})$$

for even dimensions  $D = 4 + \delta \geq 4$ .

## B The NJL model in $D(> 4)$ dimensions

We consider the Nambu–Jona-Lasinio (NJL) model<sup>10</sup> in  $D(> 4)$  dimensions,

$$\mathcal{L} = \bar{\psi} i \Gamma^M \partial_M \psi + \frac{G}{2N} (\bar{\psi} \psi)^2. \quad (\text{B.1})$$

---

<sup>10</sup> In order to avoid the complexity associated with the definition of the continuous chiral symmetry in  $D$  dimensions, we discuss in this appendix the NJL model which only has the discrete chiral symmetry (may be called “Gross-Neveu” model) .

The gap equation is obtained from the self-consistency condition for the dynamical mass  $m$ . In the large  $N$  limit, we find

$$\begin{aligned} m &= \frac{\eta G \Lambda^{D-2}}{(4\pi)^{D/2} \Gamma(D/2)} \int_0^{\Lambda^2} dp_E^2 \left( \frac{p_E^2}{\Lambda^2} \right)^{D/2-1} \frac{m}{p_E^2 + m^2}, \\ &= g \int_0^1 dz z^{D/2-1} \frac{m}{z + m^2/\Lambda^2}, \end{aligned} \quad (\text{B.2})$$

where  $\eta (= 2^{D/2})$  represents the dimension of the spinor representation of  $SO(1, D-1)$ . The dimensionless NJL coupling  $g$  is defined by  $g \equiv (4\pi)^{-D/2} \eta G \Lambda^{D-2} / \Gamma(D/2)$ . Expanding the integrand of Eq.(B.2) in terms of  $m/\Lambda$ , we obtain

$$\frac{1}{g} = \frac{1}{D/2 - 1} - \frac{1}{D/2 - 2} \frac{m^2}{\Lambda^2} + \dots$$

The scaling behavior of the NJL model in  $D(> 4)$  dimensions is then given by

$$\frac{1}{g_{\text{crit}}} - \frac{1}{g} = \frac{2}{D-4} \frac{m^2}{\Lambda^2}, \quad g_{\text{crit}} \equiv D/2 - 1. \quad (\text{B.3})$$

In order to obtain hierarchy between  $m$  and  $\Lambda$ , we thus need a fine tuning of the NJL coupling strength in the precision of  $(m/\Lambda)^2$  level *irrespectively of  $D$  for  $D > 4$* . The situation contrasts to the NJL model in dimensions less than four where the NJL coupling needs to be close to its critical point in the precision of  $(m/\Lambda)^{D-2}$ .

## C Approximate formulas for $g_{\text{eff}}$

Eq.(7.7) can be further simplified by making several approximations. We first concentrate our attention on  $\Pi_<$ . This term depends on the renormalization scale  $\mu$  and therefore it can be minimized by taking optimized choice of  $\mu$ . We assume that appropriate  $\mu^2$  is proportional to  $-q^2$ :

$$\mu^2 = -\lambda q^2, \quad (\text{C.1})$$

with  $\lambda$  being the constant which we will determine below. Since the mass of KK-mode  $m_{\vec{n}}$  is always lighter than the renormalization scale  $\mu$  in  $\Pi_<$ , we can safely neglect  $m_{\vec{n}}$  in the following analysis. It is straightforward to evaluate  $\Pi_<$ ,

$$(4\pi)^2 \Pi_<(q^2, 0; \mu = \sqrt{-\lambda q^2}) = C_G \left[ 8 + \frac{4}{9}(2 - D) \right] - \frac{5}{9} \eta T_R N_f - b' \ln \lambda. \quad (\text{C.2})$$

This term vanishes if we take optimized value of  $\lambda$ :

$$\ln \lambda = \frac{C_G \left( -8 - \frac{4}{9}(2 - D) \right) + \frac{5}{9} \eta T_R N_f}{-b'}. \quad (\text{C.3})$$

We next turn to  $\Pi_>$ . The KK mass is always heavier than the renormalization scale  $\mu$  in this term, while  $\mu$  is proportional to  $q^2$  in the previous optimization procedure. We therefore expand  $\Pi_>$  in terms of the power of  $-q^2/m_{\vec{n}}^2$ . We find

$$(4\pi)^2 \Pi_>(q^2, m^2) = -C_G \left[ \frac{2}{3} + \frac{2-D}{60} \right] \left( \frac{-q^2}{m^2} \right) + \frac{\eta}{15} T_R N_f \left( \frac{-q^2}{m^2} \right) + \mathcal{O} \left( \left( \frac{-q^2}{m^2} \right)^2 \right). \quad (\text{C.4})$$

The sum of the KK-modes can be approximated by replacing it to an integral:

$$\sum_{\vec{k}}^{m_{\vec{k}} > \mu} \rightarrow \frac{1}{n} \frac{2\pi^{\delta/2}}{\Gamma(\delta/2)} R \int_{\mu}^{\Lambda} dm (Rm)^{\delta-1}, \quad (\text{C.5})$$

which leads to

$$\sum_{\vec{k}}^{m_{\vec{k}} > \mu} \Pi_>(q^2, m_{\vec{k}}^2) \simeq \frac{\pi R^2}{(4\pi)^2 n} \left[ -\frac{3}{5} C_G + \frac{\eta}{15} T_R N_f \right] (-q^2) \ln \frac{\Lambda^2}{\mu^2} \quad (\text{C.6})$$

for  $D = 4 + \delta$ ,  $\delta = 2$ . Combining Eqs.(C.3), (C.6) and (7.10), it is now easy to obtain Eq.(7.11). The validity of Eq.(7.11) can be confirmed also numerically. (See Fig.7.)

It should be noted that the approximation of Eq.(C.4) is not justified for  $\lambda \ll 1$ , however. In order to obtain the upper bound of  $\hat{g}_{\text{eff}}$  including such a possibility, we next evaluate the effective coupling without use of the approximations of Eq.(C.2) and Eq.(C.4). Using the approximation Eq.(C.5), we obtain a formula for the effective gauge coupling strength in six dimensions,

$$\begin{aligned} \frac{1}{\hat{g}_{\text{eff}}^2(q^2)} &= \frac{\mu^2}{(-q^2)} \left( \frac{1}{\hat{g}_{\overline{MS}}^2(\mu)} + \frac{b'}{(4\pi)^3} \right) \\ &\quad + \frac{1}{(4\pi)^3} \left( K_g(q^2, \Lambda^2) + K_b(q^2, \Lambda^2) + K_f(q^2, \Lambda^2) \right), \end{aligned} \quad (\text{C.7})$$

with

$$\begin{aligned} K_g(q^2, \Lambda^2) &\equiv 4C_G \left( \frac{5}{18} + \frac{1}{6} \ln \frac{\Lambda^2}{(-q^2)} + \frac{\Lambda^2}{(-q^2)} \tilde{K}_g(q^2, \Lambda^2) \right), \\ K_b(q^2, \Lambda^2) &\equiv -2C_G \left( \frac{31}{450} + \frac{1}{30} \ln \frac{\Lambda^2}{(-q^2)} + \frac{\Lambda^2}{(-q^2)} \tilde{K}_b(q^2, \Lambda^2) \right), \\ K_f(q^2, \Lambda^2) &\equiv -2\eta T_R N_f \left( \frac{47}{900} + \frac{1}{30} \ln \frac{\Lambda^2}{(-q^2)} + \frac{\Lambda^2}{(-q^2)} \tilde{K}_f(q^2, \Lambda^2) \right). \end{aligned}$$

The functions  $\tilde{K}_g$ ,  $\tilde{K}_b$ ,  $\tilde{K}_f$  are defined by

$$\begin{aligned} \tilde{K}_g(q^2, \Lambda^2) &\equiv \int_0^1 dx f(q^2, \Lambda^2, x), \\ \tilde{K}_b(q^2, \Lambda^2) &\equiv \int_0^1 dx (2x-1)^2 f(q^2, \Lambda^2, x), \\ \tilde{K}_f(q^2, \Lambda^2) &\equiv \int_0^1 dx x(1-x) f(q^2, \Lambda^2, x), \end{aligned}$$

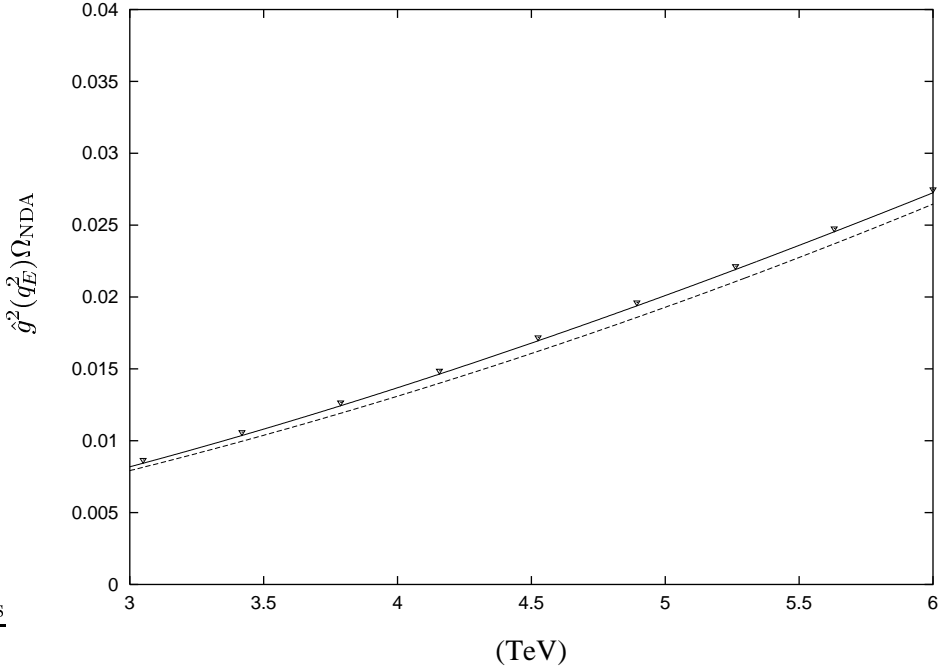


Figure 7: The graphs of the dimensionless gauge couplings. The solid line and the dashed line represent the effective coupling of Eq.(C.7) and Eq.(7.11), respectively. We also plot with the white triangle the coupling directly calculated from the definition of Eq.(7.7) without using approximation Eq.(C.5). In this graph, we took  $C_G = 3$ ,  $N_f = 0$ ,  $R^{-1} = 3\text{TeV}$ ,  $\Lambda = 6\text{TeV}$ .

with

$$f(q^2, \Lambda^2, x) \equiv (1 - x(1 - x) \frac{q^2}{\Lambda^2}) \ln \left( 1 - \frac{q^2}{\Lambda^2} x(1 - x) \right).$$

The integrals can be performed easily and we obtain (in the Euclidean region  $q^2 < 0$ ),

$$\begin{aligned} \tilde{K}_g(q^2, \Lambda^2) &= -\frac{4}{3} + \frac{5}{18} \frac{q^2}{\Lambda^2} + \frac{1}{3} \left( 4 - \frac{q^2}{\Lambda^2} \right)^{3/2} \left( \frac{\Lambda^2}{-q^2} \right)^{1/2} \tanh^{-1} \sqrt{\frac{-q^2}{4\Lambda^2 - q^2}}, \\ \tilde{K}_b(q^2, \Lambda^2) &= \frac{16}{15} \frac{\Lambda^2}{q^2} - \frac{28}{45} + \frac{31}{450} \frac{q^2}{\Lambda^2} + \frac{1}{15} \left( 4 - \frac{q^2}{\Lambda^2} \right)^{5/2} \left( \frac{\Lambda^2}{-q^2} \right)^{3/2} \tanh^{-1} \sqrt{\frac{-q^2}{4\Lambda^2 - q^2}}, \\ \tilde{K}_f(q^2, \Lambda^2) &= -\frac{4}{15} \frac{\Lambda^2}{q^2} - \frac{8}{45} + \frac{47}{900} \frac{q^2}{\Lambda^2} \\ &\quad - \frac{1}{15} \left( 4 - \frac{q^2}{\Lambda^2} \right)^{5/2} \left( 1 + \frac{q^2}{\Lambda^2} \right) \left( \frac{\Lambda^2}{-q^2} \right)^{3/2} \tanh^{-1} \sqrt{\frac{-q^2}{4\Lambda^2 - q^2}}. \end{aligned}$$

It is evident that  $\hat{g}_{\text{eff}}$  reaches its maximum at  $q^2 = -\Lambda^2$ . (See Fig. 7.) We obtain

$$K \equiv \sum_{i=g,b,f} K_i(-\Lambda^2, \Lambda^2) = C_G \left( -\frac{88}{45} + \frac{10\sqrt{5}}{3} \tanh^{-1} \frac{1}{\sqrt{5}} \right) - \frac{8\eta T_R}{45} N_f. \quad (\text{C.8})$$

Eq.(C.7) thus leads to an upper bound on  $\hat{g}_{\text{eff}}$ ,

$$\hat{g}_{\text{eff}}^2(q^2) < \frac{(4\pi)^3}{K}, \quad \text{for } 0 \leq -q^2 \leq \Lambda^2, \quad (\text{C.9})$$

where we have assumed that the  $\overline{MS}$  coupling is below its UV fixed point,

$$\hat{g}_{\overline{MS}}^2 < g_*^2 = \frac{(4\pi)^3}{-b'}. \quad (\text{C.10})$$

It should be emphasized that Eq.(C.8) is independent of the cutoff  $\Lambda$  and thus the upper bound Eq.(C.9) can be adopted for arbitrary  $\Lambda$ . In order to clarify the point, it is illuminating to define  $\hat{g}_\Lambda$  by

$$\hat{g}_\Lambda^2 \equiv \hat{g}_{\text{eff}}^2(q^2 = -\Lambda^2). \quad (\text{C.11})$$

The coupling  $\hat{g}_\Lambda$  can be regarded as a “bare parameter” of the present model. An analogue of “ $\beta$ -function” for  $\hat{g}_\Lambda$  is then given by

$$\beta(\hat{g}_\Lambda) \equiv \Lambda \frac{d}{d\Lambda} \hat{g}_\Lambda = \hat{g}_\Lambda - \frac{K}{(4\pi)^3} \hat{g}_\Lambda^3. \quad (\text{C.12})$$

The upper limit  $(4\pi)^3/K$  is thus given by the UV fixed point of the “ $\beta$ -function” Eq.(C.12).

Numerically we obtain  $K \simeq 1.63C_G - 0.71T_R N_f$ . For large  $-b'$  or large  $C_G$ , we thus find that the upper bound is roughly proportional to the UV fixed point in the  $\overline{MS}$  scheme

$$\frac{(4\pi)^3}{K} \simeq 2 \frac{(4\pi)^3}{-b'} = 2g_*^2. \quad (\text{C.13})$$

## References

- [1] V. A. Miransky, M. Tanabashi and K. Yamawaki, Phys. Lett. **B221**, 177 (1989).
- [2] V. A. Miransky, M. Tanabashi and K. Yamawaki, Mod. Phys. Lett. **A4**, 1043 (1989).
- [3] Y. Nambu, Enrico Fermi Institute Report No. 89-08, 1989; in *Proceedings of the 1989 Workshop on Dynamical Symmetry Breaking*, edited by T. Muta and K. Yamawaki (Nagoya University, Nagoya, Japan, 1990).

- [4] H. Pagels and S. Stokar, Phys. Rev. **D20**, 2947 (1979).
- [5] W. A. Bardeen, C. T. Hill and M. Lindner, Phys. Rev. **D41**, 1647 (1990).
- [6] K. Yamawaki, Prog. Theor. Phys. Suppl. **123**, 19 (1996).
- [7] N. Arkani-Hamed, H. Cheng, B. A. Dobrescu and L. J. Hall, Phys. Rev. **D62**, 096006 (2000).
- [8] B. A. Dobrescu, Phys. Lett. **B461**, 99 (1999); hep-ph/9903407.
- [9] H. Cheng, B. A. Dobrescu and C. T. Hill, Nucl. Phys. **B589**, 249 (2000).
- [10] N. Arkani-Hamed, S. Dimopoulos and G. Dvali, Phys. Lett. **B429**, 263 (1998); Phys. Rev. **D59**, 086004 (1999); I. Antoniadis, N. Arkani-Hamed, S. Dimopoulos and G. Dvali, Phys. Lett. **B436**, 257 (1998).
- [11] I. Antoniadis, Phys. Lett. **B246**, 377 (1990).
- [12] H. Abe, H. Miguchi and T. Muta, Mod. Phys. Lett. **A15**, 445 (2000).
- [13] A. B. Kobakhidze, hep-ph/9904203.
- [14] S. Raby, S. Dimopoulos and L. Susskind, Nucl. Phys. **B169**, 373 (1980).
- [15] K. R. Dienes, E. Dudas and T. Gherghetta, Phys. Lett. **B436**, 55 (1998); Nucl. Phys. **B537**, 47 (1999); I. Antoniadis, S. Dimopoulos, A. Pomarol and M. Quiros, Nucl. Phys. **B544**, 503 (1999); Z. Kakushadze, Nucl. Phys. **B548**, 205 (1999).
- [16] V. A. Miransky, Sov. J. Nucl. Phys. **38**, 280 (1983); K. Higashijima, Phys. Rev. **D29**, 1228 (1984).
- [17] V.A. Miransky and K. Yamawaki, Phys. Rev. **D55** (1997) 5051; *ibid.* **D56**, 3768 (1997).
- [18] V. A. Miransky, Nuovo Cimento, **90A**, 149 (1985).
- [19] B. Holdom, Phys. Lett. **B150**, 301 (1985); K. Yamawaki, M. Bando and K. Matumoto, Phys. Rev. Lett. **56**, 1335 (1986); T. Akiba and T. Yanagida, Phys. Lett. **B169**, 432 (1986); T. Appelquist, D. Karabali and L. C. R. Wijewardhana, Phys. Rev. Lett. **57**, 957 (1986).
- [20] K.-I. Kondo, S. Shuto and K. Yamawaki, Mod. Phys. Lett. **A6**, 3385 (1991); K.-I. Kondo, M. Tanabashi and K. Yamawaki, Prog. Theor. Phys. **89**, 1249 (1993); Nagoya/Chiba preprint DPNU-91-20/Chiba-EP-53 (July, 1991), Mod. Phys. Lett. **A8**, 2859 (1993); N.V. Krasnikov, *ibid.* **A8**, 797 (1993); M. Harada, Y. Kikukawa, T. Kugo and H. Nakano, Prog. Theor. Phys. **92**, 1161 (1994).

- [21] A. Manohar and H. Georgi, Nucl. Phys. **B234**, 189 (1984).
- [22] Z. Chacko, M.A. Luty and E. Pontón, J. High Energy Phys. **07**, 036 (2000).
- [23] K.-I. Kondo, in *Proc. 1991 Nagoya Spring School on Dynamical Symmetry Breaking, Nagoya, April 23-27, 1991*, ed. K. Yamawaki (World Scientific Pub. Co., Singapore, 1992).
- [24] Y. Kikukawa and K. Yamawaki, Phys. Lett. **B234**, 497 (1990).
- [25] M.E. Peskin, Phys. Lett. **94B**, 161 (1980).
- [26] S. Ejiri, J. Kubo and M. Murata, Phys. Rev. **D62**, 105025 (2000).
- [27] H. Kawai, M. Nio and Y. Okamoto, Prog. Theor. Phys. **88**, 341 (1992).
- [28] T. Appelquist, K. Lane and U. Mahanta, Phys. Rev. Lett. **61**, 1553 (1988).
- [29] D. Atkinson, J. Math. Phys. **28**, 2494 (1987).
- [30] T. Maskawa and H. Nakajima, Prog. Theor. Phys. **52**, 1326 (1974); *ibid.* **54**, 860 (1975); P. I. Fomin and V. A. Miransky, Phys. Lett. **B64**, 166 (1976); R. Fukuda and T. Kugo, Nucl. Phys. **B117**, 250 (1976).
- [31] H.D. Politzer, Nucl. Phys. **B117**, 397 (1976).
- [32] T. Nonoyama and M. Tanabashi, Prog. Theor. Phys. **81**, 209 (1989).
- [33] T.W. Appelquist, D. Nash and L.C.R. Wijewardhana, Phys. Rev. Lett. **60**, 2575 (1988).
- [34] W. Siegel, Phys. Lett. **84B**, 193 (1979); D.M. Capper, D.R.T. Jones and P. van Nieuwenhuizen, Nucl. Phys. **B167**, 479 (1980).
- [35] M. Hashimoto, M. Tanabashi and K. Yamawaki, in preparation.
- [36] V. P. Gusynin, A. W. Schreiber, T. Sizer and A. G. Williams, Phys. Rev. **D60**, 065007 (1999).